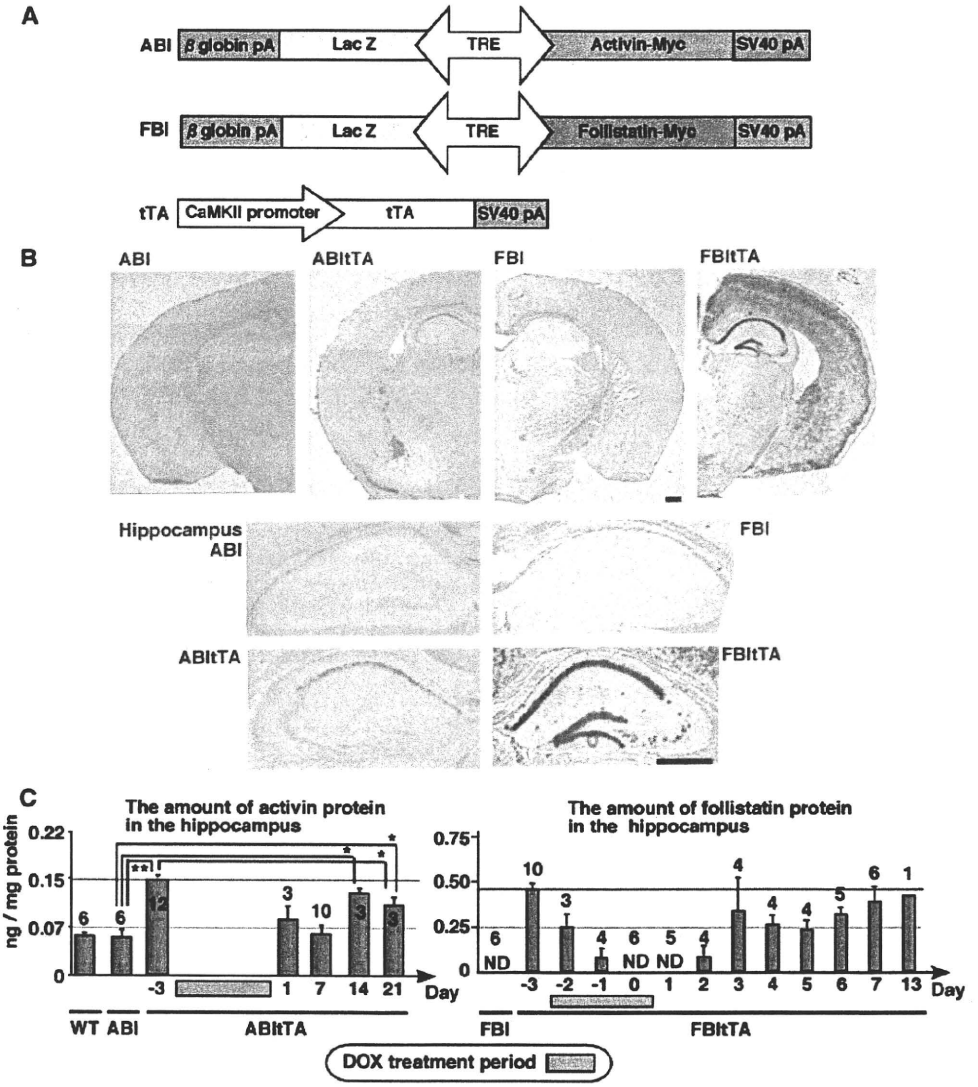

Figure 2. Generation of activin and follistatin transgenic mice using a forebrain-specific Tet-OFF system. (*A*) Schematic transgene representations of ABI (*upper*), FBI (*middle*), and tTA (*lower*) constructs. (TRE) Tetracycline response element, (tTA) tetracycline-controlled transactivtor, (pA) polyadenylation signal. (*B*) X-gal staining. (*Upper* row) Coronal brain sections from ABI, ABItTA, FBI, and FBItTA mice (10–15 wk old). (*Lower* row) Enlarged images of the hippocampus. Scale bars, 500 μm. (*C*) Measurement of activin and follistatin level using an ELISA assay with anti-activin and anti-follistatin antibodies. (Red line) Maximal levels of activin (*left* panel) or follistatin (*right* panel) in the hippocampus in the absence of DOX (10–15 wk old). Mice were fed DOX for 3 consecutive days (from noon of day −3 to noon of day 0, orange bars). The animals were then sacrificed and the hippocampus was dissected out in the afternoon of the day indicated and used for the ELISA. (ND) Not detected. The number *above* each bar indicates the number of animals used. Error bars indicate the SEM. (*) $P < 0.05$, (**) $P < 0.001$ compared with activin in the hippocampus of ABI mice in the absence of DOX, as determined by one-way ANOVA followed by Fisher's LSD test.

risk-taking behavior test, to examine the anxiety levels of FBItTA and ABItTA mice. In a risk-taking behavior test the amount of time spent in the center of an open field strongly correlates with an animal's level of anxiety (Ageta et al. 2008). The double-transgenic FBItTA and ABItTA mice showed normal anxiety-like behavior in the light–dark and risk-taking behavior tests (Supplemental Fig. S4A,B), suggesting that these mice show normal responses compared with the mutant mice used in previous work (ACM and FSM, respectively; Ageta et al. 2008). Furthermore, the performance of the double-transgenic mice (ABItTA and FBItTA) was comparable to single-transgenic mice (ABI and FBI) in sensitivity to electric footshock (Supplemental Fig. S4C). Neurogenesis in the adult hippocampus was reduced in FBItTA mice, but the reduction was less severe than in FSM mice (Supplemental Fig. S5). Therefore, the observed reduction in neurogenesis in FBItTA mice has no influence on the anxiety level. The differences in anxiety phenotype may be, perhaps, due to different follistatin levels in the brain. The FSM mice exhibited a high level of follistatin expression compared with FBItTA mice (Ageta et al. 2008).

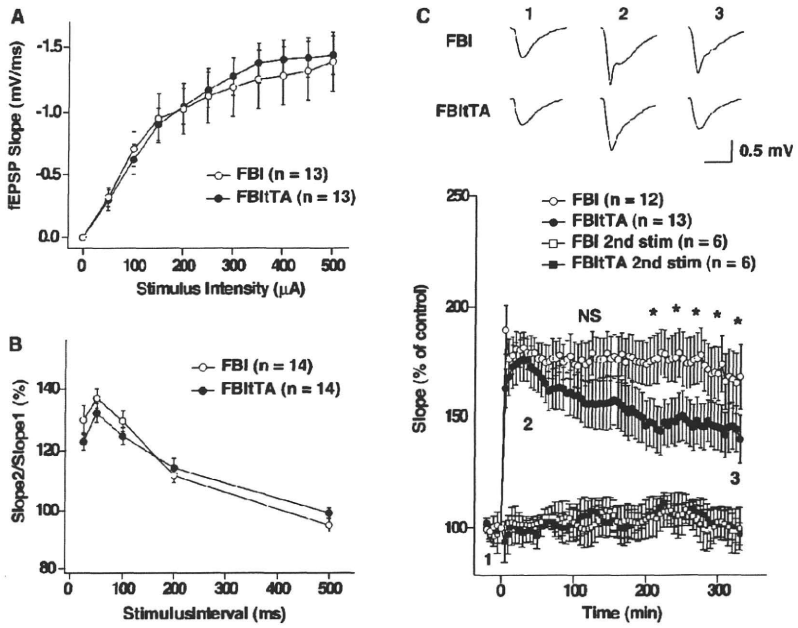

Figure 3. The maintenance of CA1 L-LTP in hippocampal slices from FBItTA mice is reduced as compared with FBI mice. (*A*) Input–output curve of fEPSP slope (millivolt [mV]/millisecond [msec]) versus stimulus (microampere [μA]) at the Schaffer collateral–CA1 pyramidal cell synapse in FBItTA and FBI mice. Data are presented as means ± SEM. (*B*) Paired-pulse ratio of fEPSPs in FBItTA and FBI mice. The initial slope of the fEPSP was measured in order to quantify the strength of the synaptic response. The ratio of the second to first response is plotted against the interstimulus interval. Data are presented as means ± SEM. (C) E-LTP and L-LTP elicited by three 100-Hz trains spaced at 20-msec intervals in FBItTA and FBI mice. The fEPSP slopes elicited by stimulation of the second independent pathway at 0.017 Hz were stable throughout the experiments. (*Insets*) Representative fEPSP traces taken at the times indicated on the graphs in C. (*) $P = 0.05$, (NS) not significant.

Once-consolidated fear memory is weakened by follistatin overexpression during the retrieval phase

We performed contextual fear-conditioning tests on FBItTA and FBI mice in the absence of DOX (Fig. 4, Experiment A). A 1-d retention test showed a significant reduction in the freezing response in FBItTA mice in Test-1 (1 d after conditioning) and Test-2 (2 d after conditioning) compared with FBI mice. There was no significant genotype effect on STM formation (Fig. 4, Experiment B). These results are consistent with the requirement for activin in L-LTP (Figs. 1A, 3C). When transgene expression was turned off by administration of DOX (orange bars, Fig. 4) for 3 consecutive days prior to conditioning, the 1-d memory of FBItTA mice was normal (Fig. 4, Experiment C, Test-1). This result indicates that follistatin expression during development of FBItTA mice did not affect the formation of neuronal circuits that are involved in contextual fear conditioning. Thus, LTM consolidation, but not short-term memory, requires activin activity in the forebrain.

One-week memory tests measured a comparable freezing behavior in FBItTA and FBI mice when DOX was administered for 3 consecutive days before conditioning (Fig. 4, Experiment D, Test-1 [indicated as T1]; Test-1 was performed 7 d after conditioning). Thus, the 1-wk memory was normal despite the inhibition of activin signaling during maintenance and retrieval, from day 3 to day 7, when fear conditioning was carried out in the absence of transgene expression. Importantly, when the same animals were retested for freezing behavior 24 h later, the FBItTA mice showed significantly less freezing response compared with the FBI mice (Fig. 4, Experiment D, Test-2 [T2]; Test-2 was performed 8 d after conditioning). In contrast, there was no difference in freezing between FBItTA and FBI mice in Test-2 of Experiment C. In these two paradigms (Experiments C and D), the interval between conditioning and Test-2 was the same (8 d). One of the major differences in the experimental paradigm was that in Experiment D the forebrain activin signal was inhibited during the retrieval period (Test-1), while in Experiment C it was not. We performed an additional experiment that is based on Experiment D. In this paradigm, mice were continuously fed on DOX to suppress the follistatin expression during the maintenance and retrieval phase (Experiment F). We did not observe a significant genotype effect in either Test-1 or -2 of Experiment F. Thus, inhibition of the activin signal during retrieval may result in significant suppression of the subsequent freezing response.

To examine this hypothesis, conditioned animals were reexposed to the conditioning chamber for 1 min at 4 d after the conditioning, a time at which forebrain activin was blocked (Fig. 4, Experiment E). In this experiment, we used short time reactivation because long time reactivations induce extinction (Suzuki et al. 2004). The other procedures were essentially the same as in Experiment D. We observed that injection of the protein synthesis inhibitor anisomycin 30 min after the reactivation into wild-type mice, which had been subjected to the same experimental paradigm as in Experiment E, resulted in a reduction in the freezing response in Test 24 h later (Supplemental Fig. S6). In experiment E, we observed a significant reduction in freezing level in Test-1 (7 d after conditioning) of FBItTA mice compared with FBI mice, strongly suggesting that the reactivation of fear memory in the absence of forebrain activin activity caused the decreased freezing response.

Fear memory is influenced by activin overexpression during the retrieval phase

A complementary experiment with ABItTA and ABI mice strengthens the idea that forebrain activin is important for proper processing of fear memory following memory reactivation (retrieval) (Fig. 5, Experiment G). In this experiment, we used a relatively weak conditioning protocol to avoid saturation of freezing response. A 3-wk memory test showed a normal freezing response in ABItTA mice compared with ABI mice (Test-1 in Experiment G, 21 d after conditioning), when the activin level was reduced to the basal level at conditioning by DOX administration. However, when the freezing response of the animals was tested 24 h later, ABItTA mice showed significantly more freezing than ABI mice (Test-2 in Experiment G, 22 d after conditioning). Furthermore, we observed a significant increase in freezing level in Test (21 d after conditioning) of ABItTA compared with their

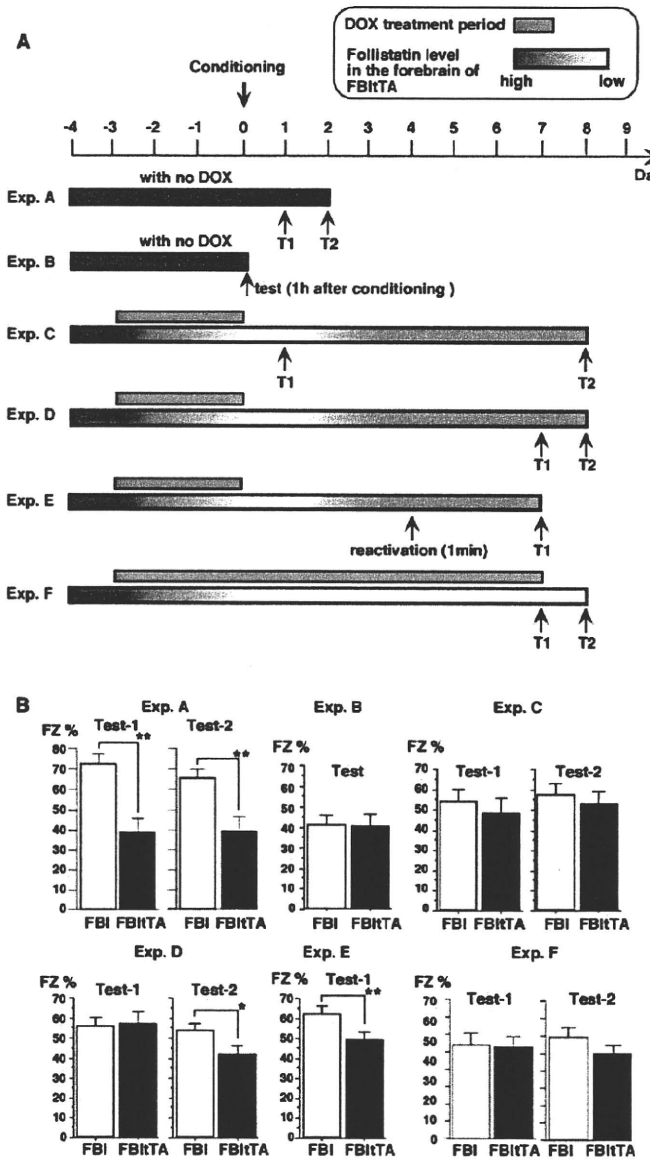

Figure 4. Once-consolidated fear memory is weakened by follistatin overexpression during the retrieval phase. (*A*) Experimental schedule. The horizontal axis indicates the time line. Mice were fed DOX for 3 consecutive days before conditioning (from noon of day −3 to noon of day 0), as indicated (orange bars). The density of blue color indicates the predicted level of follistatin in the forebrain. The numbers of mice used were: Experiment A (FBItTA, $n = 8$; FBI, $n = 9$); Experiment B (FBItTA, $n = 10$; FBI, $n = 10$); Experiment C (FBItTA, $n = 8$; FBI, $n = 11$); Experiment D (FBItTA, $n = 10$; FBI, $n = 10$); Experiment E (FBItTA, $n = 17$; FBI, $n = 13$); Experiment F (FBItTA, $n = 11$; FBI, $n = 11$). In all the experimental paradigms, conditioning was performed in the afternoon of day 0 with the same footshock protocol. (T1) Test-1, (T2) Test-2. (*B*) Freezing response during the test period. (FZ%) Average freezing percentage during the 6-min test period. (*) $P < 0.05$, (**) $P < 0.001$, statistically significant differences between FBItTA and FBI mice, as determined by one-way ANOVA followed by Fisher's LSD test. Error bars indicate SEM. Experiment C: Two-way repeated-measures ANOVA, genotype effect, $F_{(1,17)} = 0.39$, $P = 0.539$; Test effect, $F_{(1,17)} = 2.32$, $P = 0.146$; genotype × Test, $F_{(1,17)} = 0.03$, $P = 0.8629$. Experiment D: Two-way repeated-measures ANOVA, genotype effect, $F_{(1,17)} = 0.71$, $P = 0.4$; Test effect, $F_{(1,17)} = 10.16$, $P = 0.0054$; genotype × Test, $F_{(1,17)} = 6.58$, $P = 0.02$. Experiment F: Two-way repeated-measures ANOVA, genotype effect, $F_{(1,20)} = 0.57$, $P = 0.46$; Test effect, $F_{(1,20)} = 0.10$, $P = 0.75$; genotype × Test, $F_{(1,20)} = 2.92$, $P = 0.103$.

littermates (ABI and wild-type mice) when conditioned animals were reexposed to the conditioning chamber for 1 min at 17 d after conditioning, a time at which forebrain activin was increased in ABItTA (Fig. 5, Experiment H). Taken together, these results indicate that the functional activin level in the forebrain during fear memory retrieval (in this case, Test-1 in Experiment G and reactivation in Experiment H) determines the later freezing response (Test-2 in Experiment G and Test in Experiment H).

Discussion

In this study we showed that activin is indispensable for the late maintenance of hippocampal dentate gyrus L-LTP in vivo and CA1 L-LTP in slice preparation. In the marine snail *Aplysia*, TGF-β induces long-term, but not short-term facilitation at the synapses between the sensory and motor neurons (Zhang et al. 1997). Furthermore, in rat cultured hippocampal neurons, treatment with TGF-β2, another isoform of TGF-β, affected synaptic strength and induced phosphorylation of CREB (Fukushima et al. 2007). Thus, the TGF-β family of proteins, namely, activin and TGF-β 1/2, participate not only in development but also in the neuronal plasticity of the mature CNS. In addition, we revealed the existence of prolonged E-LTP in the dentate gyrus, which on the one hand differs from E-LTP in its longer persistence and activin dependency; and on the other differs from L-LTP in its shorter persistence and lack of requirement for protein synthesis. This prolonged E-LTP has been previously described as an intermediate phase LTP (I-LTP) to occur in area CA1 of the hippocampus (Winder et al. 1998). It was found to differ from E-LTP and L-LTP in its molecular mechanisms since it is dependent on protein kinase A, does not require protein synthesis, and is suppressed by calcineurin overexpression. Although it is not clear whether dentate gyrus prolonged E-LTP and CA1 I-LTP share the same molecular mechanisms, it appears that temporally distinct tri-phase LTP is a common characteristic of hippocampal LTPs.

We demonstrated that activin in the brain is required for formation of L-LTP and consolidation of LTM (Figs. 1, 3, and 4). Follistatin failed to suppress L-LTP maintenance when it was administered 3 h after a strong HFS (Supplemental Fig. S1), and this result is consistent with the behavioral analysis of FBItTA mice. After the acquisition phase, the ectopic expression of follistatin in the maintenance phase did not affect LTM formation (Fig. 4, Experiment D, Test-1), indicating that the presence of follistatin in the maintenance phase has no effect on either L-LTP or LTM. Thus, our results strengthen the correlation between L-LTP and LTM.

There are several mechanisms by which activin may participate in L-LTP and LTM. Activin modulates dendritic spine morphology and increases the number of synaptic contacts (Shoji-Kasai et al. 2007). Activin potentiates NMDA receptor-mediated signaling cascades for long periods of time (Muller et al. 2006; Kurisaki et al. 2008). In

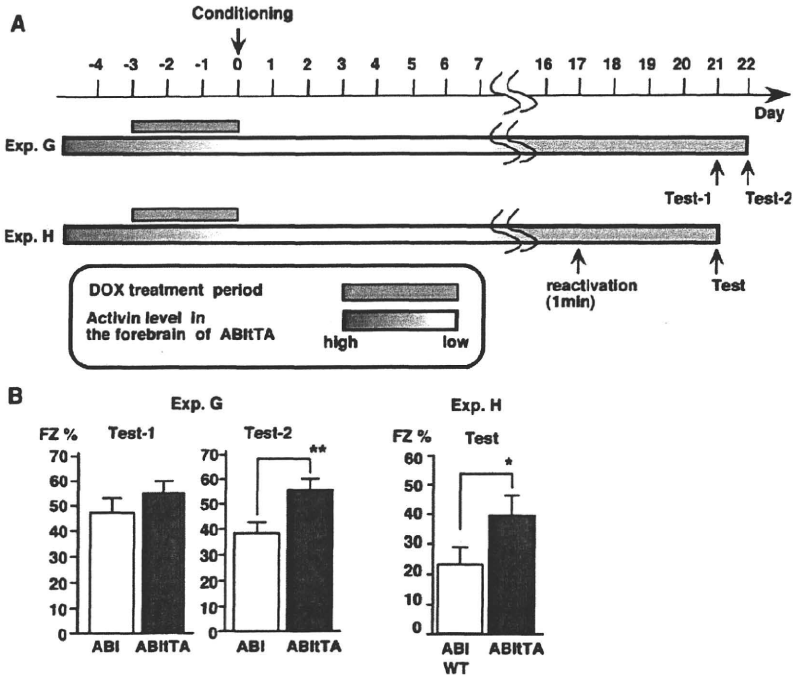

Figure 5. Fear memory is influenced by activin overexpression during the retrieval phase. (*A*) Experimental schedule. Horizontal axis indicates the time line. Mice were fed DOX for 3 consecutive days before conditioning (from noon of day −3 to noon of day 0, orange bar). The density of the red color indicates the predicted level of activin in the forebrain. Conditioning was performed in the afternoon of day 0. (*B*) Freezing response during test period. (FZ%) Average freezing percentage during the first 3 min in the 6-min test period. The numbers of mice used were: Experiment G (ABItTA, $n = 15$; ABI, $n = 16$); Experiment H (ABItTA, $n = 9$; ABI, $n = 5$; wild-type littermates, $n = 4$). (*) $P = 0.05$, (**) $P = 0.001$, statistically significant difference between ABItTA and ABI mice (Experiment G) or mixed genotypes ABI and wild group (Experiment H), as determined by one-way ANOVA followed by Fisher's LSD test. Error bars indicate SEM. (WT) Wild-type littermates. Experiment G: Two-way repeated-measures ANOVA, genotype effect, $F_{(1,23)} = 4.18$, $P = 0.0526$; Test effect, $F_{(1,23)} = 0.70$, $P = 0.410$; genotype × Test, $F_{(1,23)} = 1.63$, $P = 0.214$.

addition, activin tunes GABAergic neurotransmission (Zheng et al. 2008), which affects learning and memory (Collinson et al. 2002). All of these activin functions may contribute to the prolonged synaptic plasticity that may underlie LTM formation.

Inhibition of the activin signal during retrieval resulted in a significant suppression of subsequent expression of fear memory (Fig. 4, Experiment D, Test-2). Memory retrieval triggers two opposing processes, reconsolidation or extinction (Tronson and Taylor 2007; Quirk and Mueller 2008). Whether reconsolidation or extinction follows memory retrieval depends on the experimental conditions, such as training and retrieval conditions (Suzuki et al. 2004; Tronson and Taylor 2007). When reconsolidation dominates following memory retrieval, amnesic reagents reduce subsequent memory expression (Nader et al. 2000; Tronson and Taylor 2007). We injected the protein synthesis inhibitor anisomycin 30 min after reactivation (retrieval) into wild-type mice that had been subjected to the same experimental paradigm as in Experiment E of Figure 4. We observed a reduction in the fear response in Test (Supplemental Fig. S6). This suggests that the experimental condition used in Experiment E triggers reconsolidation. In addition, we observed that there was no significant extinction effect in control mice in Experiment D ($P = 0.7839$, one-way analysis of variance [ANOVA] with Fisher's test). On the other hand, in Experiment H in control mice, the freezing level was significantly lower than that of Test-1 in Experiment G ($P = 0.008$, one-way ANOVA with Fisher's test). As the experimental condition used in Experiment H may trigger extinction by the short-time reactivation, control mice showed a lower level of freezing in Experiment H when compared with Test-1 in Experiment G. Unfortunately, we could not record the freezing level during the reactivation phase in Experiment H because of the short period of time (reactivation took a total of 1 min, which included transportation time from the home cage to the test chamber located in a soundproof room [15 sec], exposure time to the chamber [30 sec], and another transportation time from the chamber to the home cage [15 sec]). Taken together, the suppression of freezing observed in Experiments D and E could be caused by inhibition of reconsolidation. On the other hand, the constant level of freezing in ABItTA mice observed in Experiments G and H could be attributed to the inhibition of extinction. In any case, the level of activin in the brain during the retrieval phase plays a key role in the maintenance of LTM.

Recent studies show that fear memory can be weakened by inhibiting CREB (Kida et al. 2002), *zif*268 (Lee et al. 2004), C/EBPβ (Tronel et al. 2005), ERK (Kelly et al. 2003), or PKA (Tronson et al. 2006) during memory retrieval. The present study shows that activin inhibition during memory retrieval suppresses previously consolidated fear memories. Thus, activin signaling could be a promising target for treatment of disorders that are based upon strong traumatic memories, such as post traumatic stress disorder and phobias.

Materials and Methods

Animals

Male Wistar rats (5–6 mo old) were used for the LTP experiments. All procedures involving the use of animals complied with the National Institutes of Health guidelines for the care and use of laboratory animals and were approved by the Animal Care and Use Committee of the Mitsubishi Kagaku Institute of Life Sciences.

All behavior experiments were conducted in a blind fashion on male mice. Two weeks before behavioral analysis, animals were housed individually in plastic cages and maintained on a 12:12 h light:dark cycle. Food and water were provided ad libitum. The mice were handled daily for 7 d before behavioral analysis.

Dentate gyrus LTP in vivo

Dentate gyrus LTP experiments with urethane-anesthetized rats were carried out as described previously (Ikegami et al. 1996; Inokuchi et al. 1996; Ikegami and Inokuchi 2000; Fukazawa et al. 2003) with the following modifications: To avoid subjecting the animals to unnecessary pain, the wound margins were locally infiltrated and anesthetized with 2% xylocaine. The monopolar recording electrode was then inserted into the hilus of the dentate gyrus (4.0 mm posterior, 2.8 mm lateral, 3.0 mm ventral to the dura). The bipolar stimulating electrode was positioned ipsilaterally to the medial perforant pathway (8.0 mm posterior, 4.0 mm lateral, 3.0 mm ventral to the dura). The stimulus intensities

were set at the current that evoked 50% of the maximum population spike amplitude and were kept constant throughout the experiment. Test stimuli were delivered at 30-sec intervals to record the fEPSP. After recording a stable basal transmission for 30 min, an HFS was delivered and the fEPSPs were recorded for 24 h. In the follistatin infusion experiments, a strong HFS was used, which consisted of five trains of 400 pulses at 400 Hz at 2-min intervals. In the activin infusion experiments, we used a weak HFS, which consisted of 50 pulses at 100 Hz. In most experiments, an HFS (100 pulses at 100 Hz) was given after the 24-h recording period and responses were recorded for a further 60 min. The initial EPSP slopes are shown as a percentage of the mean value obtained in the 15 min immediately prior to delivery of the HFS. To determine whether the magnitude of LTP differed among the groups, responses from the last 15 min block of recording for each 60 min period were compared statistically. The data are expressed as means ± standard error of the mean (SEM) and were analyzed by one-way or two-way ANOVA followed by Fisher's least significant difference (LSD) test.

Drug infusions

Follistatin and activin were prepared from bovine follicular fluid as described previously (Nakamura et al. 1992). Follistatin and activin were dissolved in 50 mM phosphate-buffered saline (PBS, pH 7.4) containing 0.125% bovine serum albumin (BSA). Anisomycin (Sigma-Aldrich) was dissolved in equimolar HCl, diluted with saline, and adjusted to pH 7.4 with NaOH.

In the experiments shown in Figure 1, activin, follistatin, anti-activin A, or the vehicle solution (PBS containing 0.125% BSA) were infused 45 min prior to the first HFS delivery. Anisomycin was infused 60 min prior to the first HFS delivery. The drugs were infused into the left lateral ventricle (1.0 mm posterior to the bregma, 1.8 mm lateral, 3.5 mm ventral to the dura) ipsilateral to the recording site with a 27-gauge microsyringe. The drug solution (total volume of 2.0 μL) was infused at a rate of 0.5 μL/min and the microsyringe was left in place for 5 min after the injection.

In the experiments shown in Figure 2, activin, follistatin, or vehicle solution (PBS containing 0.125% BSA) were injected at 1 or 3 h after the first HFS delivery using a cannula device (brain infusion kit, Alzet) that had been implanted into the lateral ventricle and connected to a microsyringe. The drug solution (total volume of 2.0 μL) was infused at a rate of 0.5 μL/min.

Transgenic mice

To generate the transgene vectors, we used the pBI-G plasmid (Clontech), which has a multiple cloning site, TRE promoter, a LacZ gene, and β-globin poly A and SV40 poly A sequences (Fig. 2A). We introduced a *XhoI-FseI-PacI-HindIII-AscI* site to the *NotI* site of pBI-G and refer to this plasmid as pBI-G2. Coding sequences for *activin* and *follistatin* were isolated by *AscI-XhoI* digestion from the pCaM-activin-Myc and pCaM-follistatin-Myc plasmids (Ageta et al. 2008), respectively, and inserted into the *AscI-XhoI*-digested pBI-G2 to generate the pBI-G2-activin-Myc and pBI-G2-follistatin-Myc plasmids. *AseI* fragments were isolated from pBI-G2-activin-Myc or pBI-G2-follistatin-Myc and microinjected into the pronuclei of one-cell embryos of C57BL/6J mice to produce transgenic mice (Hogan et al. 1994). Microinjected embryos were transferred to the oviducts of pseudopregnant females. We purchased tTA mice (B6; CBA-TgN [CamK2tTA]-1Mmay) from the Jackson Laboratory (Maine), and these mice were backcrossed for six generations to the C57BL/6J background mice before crossing with FBI mice. Littermate single transgenic mice, FBI and ABI, were used as controls against FBItTA and ABItTA mice, respectively. Male mice 70–100 d old were used for behavioral analysis. Mice were fed DOX (Sigma, D-9891, 6 mg/g food) for 3 consecutive days where indicated. The founder mice and offspring were identified by Southern blot analysis using the LacZ gene as a probe and PCR analysis using two independent transgene-specific primer pairs. Forward (f) and reverse (r) PCR primers for genotyping were as follows: tTA, f-5′-TGCCGCCA TTATTACGACAA-3′ and r-5′-TCCTCGCCGTCTAAGTGGAG-3′, f-5′-TTGCGTATTGGAAGATCAAG-3′ and r-5′-GATGGTAGACCC GTAATTGT-3′; FBI, f-5′-TATTCGCGTAAGGAAATCCA-3′ and r-5′-GCCGAGTTTGTCAGAAAGCA-3′, f-5′-TCCTTGCTCAGTTCG GTCTT-3′ and r-5′-CCCCACTTTGCGTTTCTTCT-3′; ABI, f-5′-TA TTCGCGTAAGGAAATCCA-3′ and r-5′-GCCGAGTTTGTCAGAA AGCA-3′, f-5′-ATCTCCACATACCCGTTCTC-3′ and r-5′-CTCCC CACTTTGCGTTTCTT-3′.

X-gal staining

Animals were sacrificed using an overdose of anesthesia, and the brains were dissected and immediately frozen on dry ice. Cryostat sections (20-μm thick) were cut and mounted onto polylysine-coated glass slides. Sections were air-dried and stored at 80°C until use in X-gal staining. X-gal staining was carried out as described (Takeuchi et al. 1995).

CA1 LTP in slice preparation

Transversely cut hippocampal slices (300 μm) were prepared from 6- to 10-wk-old transgenic FBI and FBItTA mice, and were immersed in ice-cold artificial cerebrospinal fluid (ACSF). ACSF was saturated with 95% O_2/5% CO_2, and contained: 124 mM NaCl, 3 mM KCl, 2.4 mM $CaCl_2$, 1.2 mM $MgCl_2$, 26 mM $NaHCO_3$, 1 mM NaH_2PO_4, and 10 mM D-glucose. Slices were maintained in ACSF at room temperature for at least 1 h before recording. They were then transferred to a submersion chamber and perfused continuously (2 mL/min) with ACSF at 30°C. Schaffer collaterals were stimulated with 0.1-msec pulses using bipolar tungsten electrodes. fEPSPs were recorded extracellularly in the stratum radiatum of the CA1 region using glass microelectrodes filled with ACSF (tip resistance ca. 3–6 MΩ). Stimulus intensities were set to evoke 30%–50% of the maximal fEPSP slope. LTP was induced after recording a stable 15- to 30-min baseline fEPSP. The test pulse frequency was 0.05 Hz. For some of the experiments, two stimulating electrodes were positioned in the stratum radiatum layer to activate two independent sets of Schaffer collaterals. Pathway independence was assessed by applying two pulses with 100-msec interpulse intervals and confirming the absence of PPF between the pathways (collision test). After baseline stimulation the pathway stimulated at 0.05 Hz received one or three trains of tetanic stimulation at a frequency of 100 Hz for 1 sec at 20-sec intervals. The second pathways were stimulated at 0.017 Hz and served as a control.

Electrophysiological data were collected from two strains of transgenic mice on alternate days using PowerLab (ADInstruments) and three EPC series amplifiers (HEKA Electronik). Data were low-pass filtered (1 kHz) and sampled at 10 kHz. As a measure of synaptic strength, the initial slope of the evoked fEPSPs was calculated and expressed as percent change from the baseline mean. Error bars denote SEM values. All data were used for analysis unless the pipette resistance deviated more than 30% from baseline values or the stimulus artifact, or the shape of fiber volleys changed significantly. To test for group differences between LTP values across conditions, a Student's *t*-test was performed.

Contextual fear conditioning

After the risk-taking behavior test and light/dark test, we performed the contextual fear conditioning test on each experimental group. For the experiments in Figure 4, 2 min after putting the mice into a chamber, mice received electrical footshocks three times (0.5 mA, 1 sec, intershock interval of 1 min). After the shock they remained in the chamber for an additional 2 min. For experiments in Figure 5, 2 min after putting the mice into a chamber, mice received electrical footshocks four times (0.2 mA, 0.5 sec, intershock interval of 3 sec). After the shock they remained in the chamber for an additional 4 min. To monitor the freezing response in the test, mice were again put into the same chamber for 6 min, except for Test-1 of experiment A (duration, 1 min) in Figure 4. Freezing behavior, which is defined as no movement during consecutive 2-sec intervals, was analyzed by an automated imaging system (Muromachi Kagaku). In Experiments E and H, reactivation took a total of 1 min, which included transportation

time from the home cage to the test chamber located in a sound-proof room (15 sec), exposure time to the chamber (30 sec), and another transportation time from the chamber to the home cage (15 sec).

Sensitivity to electrical stimulation

After the contextual fear-conditioning test, we measured the sensitivity of mice to footshock (Supplemental Fig. S4C). In this test, each mouse is placed in a conditioning chamber and receives 1-sec shocks of increasing intensity (Inoue et al. 2009). The interval between shocks is 10 sec. The sequence of the current used was as follows: 0.05 mA, 0.08 mA, 0.1 mA, 0.2 mA, 0.3 mA, 0.4 mA, 0.5 mA, 0.6 mA, and 0.8 mA. The minimal level of current required to elicit the stereotypical responses of running, vocalization, and jumping was determined.

Miscellaneous methods

ELISA and analysis of neurogenesis were carried out essentially as described previously (Ageta et al. 2008). Behavioral analyses, including the risk-taking behavior and light/dark tests, were carried out as described (Ageta et al. 2008).

Acknowledgments

We thank Y. Saitoh for valuable suggestions for the behavior tests; E. Tokunaga for genotyping the transgenic mice; T. Takeuchi for advice on X-gal staining; S. Kamijo, M. Matsuo, K. Kawaguchi, and M. Yamashita for maintenance of the transgenic mice; H. Fukushima for advice on the behavior test; and members of the Inokuchi laboratory for helpful discussions. This work was supported by Special Coordinate Funds for Promoting Science and Technology, and in part by a Grant-in-Aid for Scientific Research on the Priority Area "Molecular Brain Science" from the Ministry of Education, Culture, Sports, Science, and Technology of Japan to K.I.

References

Abdipranoto-Cowley A, Park JS, Croucher D, Daniel J, Henshall S, Galbraith S, Mervin K, Vissel B. 2009. Activin A is essential for neurogenesis following neurodegeneration. *Stem Cells* **27:** 1330–1346.

Abraham WC, Mason SE, Demmer J, Williams JM, Richardson CL, Tate WP, Lawlor PA, Dragunow M. 1993. Correlations between immediate early gene induction and the persistence of long-term potentiation. *Neuroscience* **56:** 717–727.

Ageta H, Murayama A, Migishima R, Kida S, Tsuchida K, Yokoyama M, Inokuchi K. 2008. Activin in the brain modulates anxiety-related behavior and adult neurogenesis. *PLoS ONE* **3:** e1869. doi: 10.1371/journal.pone.0001869.

Andreasson K, Worley PF. 1995. Induction of β-A activin expression by synaptic activity and during neocortical development. *Neuroscience* **69:** 781–796.

Bourtchuladze R, Frenguelli B, Blendy J, Cioffi D, Schutz G, Silva AJ. 1994. Deficient long-term memory in mice with a targeted mutation of the cAMP-responsive element-binding protein. *Cell* **79:** 59–68.

Cameron VA, Nishimura E, Mathews LS, Lewis KA, Sawchenko PE, Vale WW. 1994. Hybridization histochemical localization of activin receptor subtypes in rat brain, pituitary, ovary, and testis. *Endocrinology* **134:** 799–808.

Collinson N, Kuenzi FM, Jarolimek W, Maubach KA, Cothliff R, Sur C, Smith A, Otu FM, Howell O, Atack JR, et al. 2002. Enhanced learning and memory and altered GABAergic synaptic transmission in mice lacking the α 5 subunit of the GABAA receptor. *J Neurosci* **22:** 5572–5580.

Dow AL, Russell DS, Duman RS. 2005. Regulation of activin mRNA and Smad2 phosphorylation by antidepressant treatment in the rat brain: Effects in behavioral models. *J Neurosci* **25:** 4908–4916.

Frey U, Krug M, Reymann KG, Matthies H. 1988. Anisomycin, an inhibitor of protein synthesis, blocks late phases of LTP phenomena in the hippocampal CA1 region in vitro. *Brain Res* **452:** 57–65.

Fukazawa Y, Saitoh Y, Ozawa F, Ohta Y, Mizuno K, Inokuchi K. 2003. Hippocampal LTP is accompanied by enhanced F-actin content within the dendritic spine that is essential for late LTP maintenance in vivo. *Neuron* **38:** 447–460.

Fukushima T, Liu RY, Byrne JH. 2007. Transforming growth factor-β2 modulates synaptic efficacy and plasticity and induces phosphorylation of CREB in hippocampal neurons. *Hippocampus* **17:** 5–9.

Funaba M, Murata T, Fujimura H, Murata E, Abe M, Torii K. 1997. Immunolocalization of type I or type II activin receptors in the rat brain. *J Neuroendocrinol* **9:** 105–111.

Hegde AN, Inokuchi K, Pei W, Casadio A, Ghirardi M, Chain DG, Martin KC, Kandel ER, Schwartz JH. 1997. Ubiquitin C-terminal hydrolase is an immediate-early gene essential for long-term facilitation in *Aplysia*. *Cell* **89:** 115–126.

Hirao K, Hata Y, Ide N, Takeuchi M, Irie M, Yao I, Deguchi M, Toyoda A, Sudhof TC, Takai Y. 1998. A novel multiple PDZ domain-containing molecule interacting with *N*-methyl-D-aspartate receptors and neuronal cell adhesion proteins. *J Biol Chem* **273:** 21105–21110.

Hogan B, Beddington R, Constantini F, Lacy E. 1994. *Manipulating the mouse embryo: A laboratory manual*. Cold Spring Harbor Laboratory Press, Cold Spring Harbor, New York.

Ikegami S, Inokuchi K. 2000. Antisense DNA against calcineurin facilitates memory in contextual fear conditioning by lowering the threshold for hippocampal long-term potentiation induction. *Neuroscience* **98:** 637–646.

Ikegami S, Kato A, Kudo Y, Kuno T, Ozawa F, Inokuchi K. 1996. A facilitatory effect on the induction of long-term potentiation in vivo by chronic administration of antisense oligodeoxynucleotides against catalytic subunits of calcineurin. *Brain Res Mol Brain Res* **41:** 183–191.

Inokuchi K, Kato A, Hiraia K, Hishinuma F, Inoue M, Ozawa F. 1996. Increase in activin βA mRNA in rat hippocampus during long-term potentiation. *FEBS Lett* **382:** 48–52.

Inoue N, Nakao H, Migishima R, Hino T, Matsui M, Hayashi F, Nakao K, Manabe T, Aiba A, Inokuchi K. 2009. Requirement of the immediate early gene *vesl-1S/homer-1a* for fear memory formation. *Mol Brain* **2:** 7. doi: 10.1186/1756-6606-2-7.

Kato A, Ozawa F, Saitoh Y, Hirai K, Inokuchi K. 1997. *vesl*, a gene encoding VASP/Ena family related protein, is upregulated during seizure, long-term potentiation and synaptogenesis. *FEBS Lett* **412:** 183–189.

Kelly A, Laroche S, Davis S. 2003. Activation of mitogen-activated protein kinase/extracellular signal-regulated kinase in hippocampal circuitry is required for consolidation and reconsolidation of recognition memory. *J Neurosci* **23:** 5354–5360.

Kida S, Josselyn SA, de Ortiz SP, Kogan JH, Chevere I, Masushige S, Silva AJ. 2002. CREB required for the stability of new and reactivated fear memories. *Nat Neurosci* **5:** 348–355.

Kitamura T, Saitoh Y, Takashima N, Murayama A, Niibori Y, Ageta H, Sekiguchi M, Sugiyama H, Inokuchi K. 2009. Adult neurogenesis modulates the hippocampus-dependent period of associative fear memory. *Cell* **139:** 814–827.

Kurisaki A, Inoue I, Kurisaki K, Yamakawa N, Tsuchida K, Sugino H. 2008. Activin induces long-lasting *N*-methyl-D-aspartate receptor activation via scaffolding PDZ protein activin receptor interacting protein 1. *Neuroscience* **151:** 1225–1235.

Lee JL, Everitt BJ, Thomas KL. 2004. Independent cellular processes for hippocampal memory consolidation and reconsolidation. *Science* **304:** 839–843.

Lee SH, Choi JH, Lee N, Lee HR, Kim JI, Yu NK, Choi SL, Kim H, Kaang BK. 2008. Synaptic protein degradation underlies destabilization of retrieved fear memory. *Science* **319:** 1253–1256.

Massague J. 1998. TGF-β signal transduction. *Annu Rev Biochem* **67:** 753–791.

Mather JP, Moore A, Li RH. 1997. Activins, inhibins, and follistatins: Further thoughts on a growing family of regulators. *Proc Soc Exp Biol Med* **215:** 209–222.

Mayford M, Bach ME, Huang YY, Wang L, Hawkins RD, Kandel ER. 1996. Control of memory formation through regulated expression of a CaMKII transgene. *Science* **274:** 1678–1683.

Muller MR, Zheng F, Werner S, Alzheimer C. 2006. Transgenic mice expressing dominant-negative activin receptor IB in forebrain neurons reveal novel functions of activin at glutamatergic synapses. *J Biol Chem* **281:** 29076–29084.

Nader K. 2003. Memory traces unbound. *Trends Neurosci* **26:** 65–72.

Nader K, Schafe GE, Le Doux JE. 2000. Fear memories require protein synthesis in the amygdala for reconsolidation after retrieval. *Nature* **406:** 722–726.

Nakamura T, Takio K, Eto Y, Shibai H, Titani K, Sugino H. 1990. Activin-binding protein from rat ovary is follistatin. *Science* **247:** 836–838.

Nakamura T, Asashima M, Eto Y, Takio K, Uchiyama H, Moriya N, Ariizumi T, Yashiro T, Sugino K, Titani K. 1992. Isolation and characterization of native activin B. *J Biol Chem* **267:** 16385–16389.

Nguyen PV, Abel T, Kandel ER. 1994. Requirement of a critical period of transcription for induction of a late phase of LTP. *Science* **265:** 1104–1107.

Nicoll RA, Malenka RC. 1999. Expression mechanisms underlying NMDA receptor-dependent long-term potentiation. *Ann N Y Acad Sci* **868:** 515–525.

Okada D, Ozawa F, Inokuchi K. 2009. Input-specific spine entry of soma-derived Vesl-1S protein conforms to synaptic tagging. *Science* **324:** 904–909.

Pangas SA, Woodruff TK. 2000. Activin signal transduction pathways. *Trends Endocrinol Metab* **11:** 309–314.

Quirk GJ, Mueller D. 2008. Neural mechanisms of extinction learning and retrieval. *Neuropsychopharmacology* **33:** 56–72.

Rioult-Pedotti MS, Friedman D, Donoghue JP. 2000. Learning-induced LTP in neocortex. *Science* **290:** 533–536.

Rodrigues SM, Schafe GE, LeDoux JE. 2004. Molecular mechanisms underlying emotional learning and memory in the lateral amygdala. *Neuron* **44:** 75–91.

Rogan MT, Staubli UV, LeDoux JE. 1997. Fear conditioning induces associative long-term potentiation in the amygdala. *Nature* **390:** 604–607.

Sekiguchi M, Hayashi F, Tsuchida K, Inokuchi K. 2009. Neuron type-selective effects of activin on development of the hippocampus. *Neurosci Lett* **452:** 232–237.

Shoji H, Tsuchida K, Kishi H, Yamakawa N, Matsuzaki T, Liu Z, Nakamura T, Sugino H. 2000. Identification and characterization of a PDZ protein that interacts with activin type II receptors. *J Biol Chem* **275:** 5485–5492.

Shoji-Kasai Y, Ageta H, Hasegawa Y, Tsuchida K, Sugino H, Inokuchi K. 2007. Activin increases the number of synaptic contacts and the length of dendritic spine necks by modulating spinal actin dynamics. *J Cell Sci* **120:** 3830–3837.

Silva AJ, Kogan JH, Frankland PW, Kida S. 1998. CREB and memory. *Annu Rev Neurosci* **21:** 127–148.

Squire LR, Barondes SH. 1973. Memory impairment during prolonged training in mice given inhibitors of cerebral protein synthesis. *Brain Res* **56:** 215–225.

Sugino H, Sugino K, Hashimoto O, Shoji H, Nakamura T. 1997. Follistatin and its role as an activin-binding protein. *J Med Invest* **44:** 1–14.

Suzuki A, Josselyn SA, Frankland PW, Masushige S, Silva AJ, Kida S. 2004. Memory reconsolidation and extinction have distinct temporal and biochemical signatures. *J Neurosci* **24:** 4787–4795.

Takeuchi T, Yamazaki Y, Katoh-Fukui Y, Tsuchiya R, Kondo S, Motoyama J, Higashinakagawa T. 1995. Gene trap capture of a novel mouse gene, *jumonji*, required for neural tube formation. *Genes & Dev* **9:** 1211–1222.

Tretter YP, Hertel M, Munz B, ten Bruggencate G, Werner S, Alzheimer C. 2000. Induction of activin A is essential for the neuroprotective action of basic fibroblast growth factor in vivo. *Nat Med* **6:** 812–815.

Tronel S, Milekic MH, Alberini CM. 2005. Linking new information to a reactivated memory requires consolidation and not reconsolidation mechanisms. *PLoS Biol* **3:** e293. doi: 10.1371/journal.pbio.0030293.

Tronson NC, Taylor JR. 2007. Molecular mechanisms of memory reconsolidation. *Nat Rev Neurosci* **8:** 262–275.

Tronson NC, Wiseman SL, Olausson P, Taylor JR. 2006. Bidirectional behavioral plasticity of memory reconsolidation depends on amygdalar protein kinase A. *Nat Neurosci* **9:** 167–169.

Winder DG, Mansuy IM, Osman M, Moallem TM, Kandel ER. 1998. Genetic and pharmacological evidence for a novel, intermediate phase of long-term potentiation suppressed by calcineurin. *Cell* **92:** 25–37.

Yao I, Takagi H, Ageta H, Kahyo T, Sato S, Hatanaka K, Fukuda Y, Chiba T, Morone N, Yuasa S, et al. 2007. SCRAPPER-dependent ubiquitination of active zone protein RIM1 regulates synaptic vesicle release. *Cell* **130:** 943–957.

Ying SY, Zhang Z, Furst B, Batres Y, Huang G, Li G. 1997. Activins and activin receptors in cell growth. *Proc Soc Exp Biol Med* **214:** 114–122.

Zhang F, Endo S, Cleary LJ, Eskin A, Byrne JH. 1997. Role of transforming growth factor-β in long-term synaptic facilitation in *Aplysia*. *Science* **275:** 1318–1320.

Zheng F, Adelsberger H, Muller MR, Fritschy JM, Werner S, Alzheimer C. 2008. Activin tunes GABAergic neurotransmission and modulates anxiety-like behavior. *Mol Psychiatry* **14:** 332–346.

Received October 11, 2009; accepted in revised form February 5, 2010.

Regulation of Muscle Mass by Follistatin and Activins

Se-Jin Lee, Yun-Sil Lee, Teresa A. Zimmers, Arshia Soleimani, Martin M. Matzuk, Kunihiro Tsuchida, Ronald D. Cohn, and Elisabeth R. Barton

Department of Molecular Biology and Genetics (S.-J.L., Y.-S.L.) and Departments of Pediatrics and Neurology (A.S., R.D.C.), McKusick-Nathans Institute of Genetic Medicine, Johns Hopkins University School of Medicine, Baltimore, Maryland 21205; Departments of Surgery and Cell Biology and Anatomy (T.A.Z.), University of Miami Miller School of Medicine, Miami, Florida 33136; Departments of Pathology and Immunology (M.M.M.), Molecular and Human Genetics, and Molecular and Cellular Biology, Baylor College of Medicine, Houston, Texas 77030; Division for Therapies against Intractable Diseases (K.T.), Institute for Comprehensive Medical Science, Fujita Health University, Toyoake, Aichi 470-1192, Japan; and Department of Anatomy and Cell Biology (E.R.B.), University of Pennsylvania School of Dental Medicine, Philadelphia, Pennsylvania 19104

Myostatin is a TGF-β family member that normally acts to limit skeletal muscle mass. Follistatin is a myostatin-binding protein that can inhibit myostatin activity *in vitro* and promote muscle growth *in vivo*. Mice homozygous for a mutation in the *Fst* gene have been shown to die immediately after birth but have a reduced amount of muscle tissue, consistent with a role for follistatin in regulating myogenesis. Here, we show that *Fst* mutant mice exhibit haploinsufficiency, with muscles of *Fst* heterozygotes having significantly reduced size, a shift toward more oxidative fiber types, an impairment of muscle remodeling in response to cardiotoxin-induced injury, and a reduction in tetanic force production yet a maintenance of specific force. We show that the effect of heterozygous loss of *Fst* is at least partially retained in a *Mstn*-null background, implying that follistatin normally acts to inhibit other TGF-β family members in addition to myostatin to regulate muscle size. Finally, we present genetic evidence suggesting that activin A may be one of the ligands that is regulated by follistatin and that functions with myostatin to limit muscle mass. These findings potentially have important implications with respect to the development of therapeutics targeting this signaling pathway to preserve muscle mass and prevent muscle atrophy in a variety of inherited and acquired forms of muscle degeneration. (*Molecular Endocrinology* 24: 1998–2008, 2010)

Myostatin is a TGF-β family member that acts as a negative regulator of skeletal muscle mass (1). *Mstn* mRNA is first detectable in midgestation embryos in cells of the myotome compartment of developing somites and continues to be expressed in muscle throughout embryogenesis as well as in adult mice. Mice homozygous for a deletion of the *Mstn* gene exhibit dramatic and widespread increases in skeletal muscle mass, with individual muscles of *Mstn*-knockout mice weighing about twice as much as those of *wild-type* mice as a result of a combination of increased fiber number and muscle fiber hypertrophy. These findings suggested that myostatin plays two distinct roles to regulate muscle mass, one to regulate the number of muscle fibers that are formed during development and a second to regulate growth of those fibers. In this respect, selective postnatal loss of myostatin signaling as a result of either deletion of the *Mstn* gene (2, 3) or pharmacological inhibition of myostatin activity (4–7) can cause significant muscle fiber hypertrophy, demonstrating that myostatin plays an important role in regulating muscle homeostasis in adult mice. Moreover, genetic studies in cattle (8–11), sheep (12), dogs (13), and humans (14) have all shown that the function of myostatin as a negative regulator of muscle mass is highly conserved across species.

ISSN Print 0888-8809 ISSN Online 1944-9917
Printed in U.S.A.

doi: 10.1210/me.2010-0127 Received April 5, 2010. Accepted July 27, 2010.
First Published Online September 1, 2010

Abbreviations: EDL, Extensor digitorum longus; FSTL-3, follistatin-like 3; GDF, growth differentiation factor; MHC, myosin heavy chain.

The identification of myostatin and its biological function has raised the possibility that inhibition of myostatin activity may be an effective strategy for increasing muscle mass and strength in patients with inherited and acquired clinical conditions associated with debilitating muscle loss (for reviews, see Refs. 15–17). Indeed, studies employing mouse models of muscle diseases have suggested that loss of myostatin signaling has beneficial effects in a wide range of disease settings, including muscular dystrophy, spinal muscular atrophy, cachexia, steroid-induced myopathy, and age-related sarcopenia. Moreover, loss of myostatin signaling has been shown to decrease fat accumulation and improve glucose metabolism in models of metabolic diseases, raising the possibility that targeting myostatin may also have applications for diseases such as obesity and type II diabetes. As a result, there has been an extensive effort directed at understanding the mechanisms by which myostatin activity is normally regulated and on identifying the components of the myostatin-signaling pathway with the long-term goal of developing the most effective therapeutic strategies for targeting its actions.

In this regard, considerable progress has been made in terms of understanding how myostatin activity is regulated extracellularly by binding proteins (for review, see Ref. 15). One of these regulatory proteins is follistatin (FST), which is capable of acting as a potent myostatin antagonist. Follistatin has been shown to be capable of binding directly to myostatin and inhibiting its activity in receptor binding and reporter gene assays *in vitro* (18–20). Moreover, follistatin also appears to be capable of blocking endogenous myostatin activity *in vivo*, as transgenic mice overexpressing follistatin specifically in skeletal muscle have been shown to exhibit dramatic increases in muscle growth comparable to those seen in *Mstn*-knockout mice (18, 21, 22). Finally, mice homozygous for a targeted mutation in the *Fst* gene have reduced muscle mass at birth (23), consistent with a role for follistatin in inhibiting myostatin activity during embryonic development. The fact that $Fst^{-/-}$ mice die immediately after birth, however, has hampered a more detailed analysis of the role of follistatin in regulating muscle homeostasis. Here, we show that *Fst* mutant mice exhibit haploinsufficiency, with $Fst^{+/-}$ mice having significant reductions in muscle mass accompanied by corresponding decreases in muscle function and impaired muscle regeneration. Furthermore, we show that this muscle phenotype reflects a normal role for follistatin in regulating not only myostatin but also other TGF-β family members that cooperate with mysotatin to limit muscle growth, and we present genetic evidence that activin A may be one of these key cooperating ligands.

Results

Because mice homozygous for a deletion of *Fst* gene die immediately after birth (23) and because many components of the myostatin-regulatory system have shown dose-dependent effects when manipulated *in vivo*, we investigated the possibility that *Fst* mutant mice might exhibit haploinsufficiency with respect to muscle growth and function. We backcrossed the *Fst* loss-of-function mutation at least 10 times onto a C57BL/6 background and then analyzed muscle weights in $Fst^{+/-}$ mice at 10 wk of age. As shown in Table 1 and Fig. 1 (*bottom panel*), $Fst^{+/-}$ mice exhibited a clear muscle phenotype, with muscle weights in $Fst^{+/-}$ mice being lower by about 15–20% compared with those of wild-type mice. These reductions in muscle weights were highly statistically significant (P values ranged from 10^{-8} to 10^{-12}), were seen in all four muscles that were analyzed (pectoralis, triceps, quadriceps, and gastrocnemius) as well as in both males and females, and were also apparent after normalizing for total body weights (Supplemental Table 1 and Supplemental Fig. 1 published on The Endocrine Society's Journals Online web site at http://mend.endojournals.org).

These effects on muscle mass were the converse of what has been observed in mice with mutations in the *Mstn* gene and were therefore consistent with a normal role for follistatin in inhibiting myostatin activity *in vivo*. We showed previously that the higher muscle mass seen in $Mstn^{-/-}$ mice results from effects on both fiber numbers and fiber sizes (1). To determine whether both fiber numbers and fiber sizes are also affected by the *Fst* mutation, we carried out morphometric analysis of sections of the gastrocnemius muscle. As shown in Table 2, total fiber number in the gastrocnemius appeared to be unaffected in $Fst^{+/-}$ mice compared with *wild-type* controls. One difference clearly evident in hematoxylin and eosin-stained sections, however, was the increased proportion of smaller, more darkly stained fibers in muscles of $Fst^{+/-}$ mice (Fig. 2A), raising the possibility that heterozygous loss of *Fst* might affect fiber type distribution. In this respect, previous studies have shown that loss of myostatin affects the relative proportions of the different fiber types, with $Mstn^{-/-}$ mice having a decreased number of type I fibers and an increased number of type II fibers in the soleus as well as a shift in the distribution of type II fibers toward more of the glycolytic type IIb fibers in the extensor digitorum longus (EDL) (24–27). Fiber type analysis of the gastrocnemius muscle of $Fst^{+/-}$ mice revealed an opposite shift toward more oxidative fibers. In particular, the number of oxidative type I fibers was increased significantly in the gastrocnemius muscle of $Fst^{+/-}$ mice (Table 2), and most of the small darkly

TABLE 1. Muscle weights of mutant mice

		Body weight (g)	Muscle weights (mg)			
			Pectoralis	Triceps	Quadriceps	Gastrocnemius
Males						
Wild type	(n=36)	24.0 ± 0.3	74.5 ± 1.0	94.8 ± 1.2	193.3 ± 2.5	137.5 ± 1.7
$Fst^{+/-}$	(n=15)	23.3 ± 0.7	60.7 ± 1.0[a]	78.3 ± 1.4[a]	157.4 ± 3.0[a]	118.2 ± 2.0[a]
$Fstl3^{-/-}$	(n=23)	25.3 ± 0.6	77.2 ± 1.7	97.9 ± 1.6	200.7 ± 3.8	138.2 ± 2.1
$Mstn^{+/-}$	(n=17)	27.6 ± 0.4	97.4 ± 1.6	123.2 ± 2.4	252.6 ± 4.5	181.2 ± 3.9
$Mstn^{+/-}$, $Fst^{+/-}$	(n=12)	26.0 ± 0.4[b]	79.3 ± 1.5[c]	100.0 ± 2.0[c]	197.8 ± 5.3[c]	147.4 ± 3.2[c]
$Mstn^{-/-}$	(n= 8)	33.8 ± 0.9	215.1 ± 7.9	231.8 ± 7.3	407.1 ± 12.1	302.0 ± 10.3
$Mstn^{-/-}$, $Fst^{+/-}$	(n=10)	31.0 ± 1.3	174.3 ± 10.0[d]	206.7 ± 10.4	352.6 ± 17.3[e]	274.4 ± 13.4
$inh\beta A^{+/-}$	(n=21)	25.0 ± 0.4[f]	80.8 ± 1.2[a]	104.0 ± 1.6[a]	215.0 ± 3.8[a]	152.3 ± 2.2[a]
$inh\beta B^{+/-}$	(n=13)	24.3 ± 0.5	73.5 ± 1.7	95.8 ± 2.5	190.1 ± 3.9	134.6 ± 2.2
$inh\beta B^{-/-}$	(n=15)	24.7 ± 0.4	78.9 ± 1.7[f]	100.4 ± 2.5[f]	201.3 ± 5.0	139.1 ± 2.9
$inh\beta C^{+/-}$, $\beta E^{+/-}$	(n=12)	24.8 ± 1.2	76.2 ± 3.3	95.8 ± 2.6	192.2 ± 8.3	133.9 ± 5.7
$inh\beta C^{-/-}$, $\beta E^{-/-}$	(n=18)	25.0 ± 0.4[f]	76.9 ± 1.3	96.8 ± 1.9	196.9 ± 3.3	138.6 ± 2.0
Females						
Wild type	(n=22)	19.0 ± 0.2	48.3 ± 0.8	69.5 ± 0.9	146.2 ± 1.8	102.5 ± 1.2
$Fst^{+/-}$	(n=14)	17.2 ± 0.4[a]	39.1 ± 0.9[a]	56.6 ± 1.0[a]	115.2 ± 2.0[a]	84.7 ± 1.7[a]
$Fstl3^{-/-}$	(n=29)	19.1 ± 0.3	50.6 ± 0.8[f]	72.5 ± 0.9[f]	149.4 ± 1.8	100.7 ± 1.1
$Fst^{+/-}$, $Fstl3^{+/-}$	(n= 9)	16.3 ± 0.5[a]	37.3 ± 1.6[a]	57.0 ± 2.2[a]	113.9 ± 4.6[a]	82.9 ± 2.8[a]
$Fst^{+/-}$, $Fstl3^{-/-}$	(n= 7)	16.9 ± 0.6[g]	36.9 ± 1.4[a]	57.3 ± 1.5[a]	116.1 ± 4.0[a]	80.3 ± 2.6[a]
$Mstn^{+/-}$	(n=13)	22.0 ± 0.4	64.2 ± 1.0	90.5 ± 1.1	185.1 ± 2.3	130.5 ± 1.8
$Mstn^{+/-}$, $Fst^{+/-}$	(n=10)	20.6 ± 0.4[h]	52.3 ± 1.3[c]	74.6 ± 2.0[c]	152.6 ± 3.5[c]	111.7 ± 2.2[c]
$Mstn^{-/-}$	(n=13)	24.5 ± 0.4	111.0 ± 2.3	148.5 ± 1.8	276.8 ± 4.2	195.8 ± 2.4
$Mstn^{-/-}$, $Fst^{+/-}$	(n=17)	24.3 ± 0.3	94.4 ± 1.6[i]	139.2 ± 1.6[i]	251.2 ± 3.4[i]	186.9 ± 2.4[e]
$inh\beta A^{+/-}$	(n=20)	19.4 ± 0.2	52.4 ± 0.9[a]	73.3 ± 1.3[f]	155.3 ± 2.2[g]	109.3 ± 1.7[g]
$inh\beta B^{+/-}$	(n=15)	19.8 ± 0.4	50.5 ± 0.8[f]	70.0 ± 1.2	147.5 ± 2.7	100.8 ± 1.8
$inh\beta B^{-/-}$	(n=12)	20.0 ± 0.6	51.8 ± 1.4[f]	69.9 ± 1.2	144.3 ± 3.3	100.8 ± 2.2
$inh\beta C^{+/-}$, $\beta E^{+/-}$	(n=15)	18.5 ± 0.7	49.2 ± 1.5	69.4 ± 2.3	141.0 ± 5.5	97.5 ± 4.5
$inh\beta C^{-/-}$, $\beta E^{-/-}$	(n=25)	19.1 ± 0.2	49.9 ± 0.9	70.5 ± 1.0	150.4 ± 2.1	103.0 ± 1.4

[a] $P < 0.001$ *vs. wild type*; [b] $P < 0.01$ *vs.* $Mstn^{+/-}$; [c] $P < 0.001$ *vs.* $Mstn^{+/-}$; [d] $P < 0.01$ *vs.* $Mstn^{-/-}$; [e] $P < 0.05$ *vs.* $Mstn^{-/-}$; [f] $P < 0.05$ *vs. wild-type*; [g] $P < 0.01$ *vs. wild type*; [h] $P < 0.05$ *vs.* $Mstn^{+/-}$; [i] $P < 0.001$ *vs.* $Mstn^{-/-}$.

stained fibers that appeared to be increased in number in $Fst^{+/-}$ mice corresponded to mixed glycolytic/oxidative type IIa fibers, representing a further shift away from glycolytic type IIb fibers (Fig. 2A). We observed similar trends toward more oxidative fibers in other muscles as well, with the appearance of a significant percentage of type I fibers in the EDL ($P < 0.001$) (Fig. 2B) and an approximately 5% shift from type IIa fibers to type I fibers in the soleus, although these latter data did not reach statistical significance.

To determine whether differences in fiber sizes could account for the differences in muscle weights between $Fst^{+/-}$ and *wild-type* mice, we measured fiber diameters in representative sections of the gastrocnemius muscle. As shown in Fig. 2C and Table 2, the distribution of fiber diameters was shifted toward smaller fibers in the gastrocnemius muscle of $Fst^{+/-}$ mice compared with that of *wild-type* mice. Significantly, the shift in the distribution toward smaller fibers was observed not only in type II fibers but also in type I fibers. Hence, the overall decrease in the weight of the gastrocnemius muscle of $Fst^{+/-}$ mice appeared to result from a combination of an increase in the proportion of fiber types that are generally smaller in size and a decrease in mean fiber diameter for each fiber type.

We also analyzed the effects of heterozygous loss of *Fst* on muscle function. Previous studies have shown that inhibition of myostatin activity in mice results in increased muscle force (4). To determine whether the lower muscle mass seen in $Fst^{+/-}$ mice results in lower muscle force production, we carried out force measurements on isolated muscles. As shown in Fig. 3, twitch and tetanic force were lower in $Fst^{+/-}$ mice by 27% and 26%, respectively, in the soleus and by 28% and 17%, respectively, in the EDL, which was commensurate with the reduction in cross-sectional area. Hence, the lower muscle weights seen in $Fst^{+/-}$ mice appear to result in corresponding decreases in tetanic force production, with no statistically significant changes in specific force.

Loss of myostatin has been shown to affect not only muscle mass and strength but also the ability of the muscle to regenerate. In particular, loss of myostatin activity has been shown to result in an enhanced regenerative response to both chronic (for reviews, see Refs. 15–17) and acute (28–30) injury. We investigated the possibility that heterozygous loss of *Fst* might have the opposite effect on muscle regeneration by examining the response of the gastrocnemius muscle to cardiotoxin-induced injury. Indeed, 21 d after induction of injury, *Fst* heterozygous mice

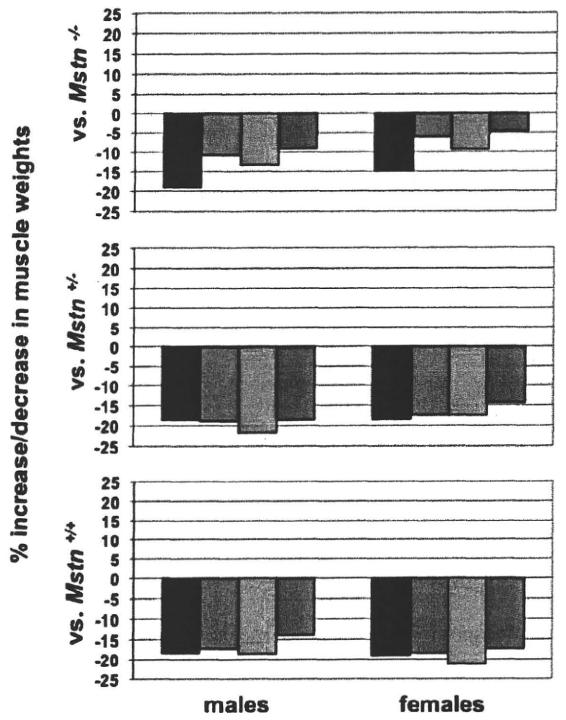

FIG. 1. Effect of heterozygous loss of *Fst* on muscle mass. *Bottom panel* shows percent decrease in muscle weights in $Fst^{+/-}$ mice compared with *wild-type* mice. *Middle panel* shows percent decrease in muscle weights in $Fst^{+/-}$, $Mstn^{+/-}$ mice compared with $Fst^{+/+}$, $Mstn^{+/-}$ mice. *Top panel* shows percent decrease in muscle weights in $Fst^{+/-}$, $Mstn^{-/-}$ mice compared with $Fst^{+/+}$, $Mstn^{-/-}$ mice. All calculations were made from the data shown in Table 1. Muscles analyzed were: pectoralis (*red*), triceps (*gray*), quadriceps (*blue*), and gastrocnemius (*green*).

showed clear deficits in muscle remodeling (Fig. 4A) with an almost 4-fold increase in the amount of muscle fibrosis as compared with *wild-type* mice (Fig. 4B). Interestingly, at 4 d after cardiotoxin-induced injury, *Fst* heterozygous mice showed no obvious difference in neonatal myosin-positive fibers compared with *wild-type* mice (Fig. 4A), suggesting that the defects in muscle remodeling may result from failed muscle maturation rather than impaired satellite cell function.

TABLE 2. Analysis of gastrocnemius/plantaris muscles

	Wild type (*n* = 3)	$Fst^{+/-}$ (n = 3)	% Difference
Total fiber number	8340 ± 323	8260 ± 521	−1.0
Type I fiber number	124 ± 30	206 ± 21	+66.1
Percentage type I fibers	1.47 ± 0.3	2.50 ± 0.2[a]	+69.7
Mean fiber diameters (μm)			
Type I fibers	32.8 ± 1.0	28.5 ± 1.2[a]	−13.0
Type IIa fibers	35.6 ± 2.4	29.9 ± 1.2[b]	−16.1
Type IIb fibers	41.9 ± 0.1	37.3 ± 1.3[a]	−11.0
All fiber types	41.0 ± 0.6	36.0 ± 1.5[a]	−12.2

[a] $P < 0.05$ *vs. wild type*; [b] $P = 0.08$ *vs. wild type*.

The fact that we could observe reductions in muscle mass in $Fst^{+/-}$ mice opened up the possibility of looking at genetic interactions between *Fst* and other genes encoding components of this regulatory system. We first looked at genetic interactions between *Fst* and *Fstl3*, which is another member of the follistatin gene family. Previous studies had shown that like follistatin, FSTL-3 (follistatin-like 3; also called FLRG) is capable of blocking myostatin activity *in vitro* (31) and promoting muscle growth when overexpressed *in vivo* (21, 22). What role FSTL-3 normally plays in regulating myostatin activity *in vivo* is unclear, however, as homozygous *Fstl3* mutant mice have been reported to have normal muscle mass (32). We investigated the possibility that the lack of a clear muscle phenotype in *Fstl3* mutant mice might reflect functional redundancy between FSTL-3 and follistatin. For these studies, we used a line of mice that we independently generated carrying a targeted deletion of *Fstl3*. As shown in Fig. 5A, we generated mice in which we deleted exons 3–5, which contains most of the protein-coding region, including both of the follistatin domains of FSTL-3. We then backcrossed this deletion allele at least seven times onto a C57BL/6 background for analysis.

Consistent with findings previously reported by others (32), mice homozygous for a deletion of *Fstl3* were viable and had relatively normal muscle weights (Table 1). To investigate possible functional redundancy, we analyzed the effect of crossing the *Fst* loss-of-function mutation onto an *Fstl3* mutant background. As shown in Table 1 and Fig. 5B, we observed no additive effects of the *Fst* and *Fstl3* mutations in terms of reducing muscle mass; that is, neither $Fst^{+/-}$, $Fstl3^{+/-}$ nor $Fst^{+/-}$, $Fstl3^{-/-}$ mice showed further reductions in muscle weights compared with $Fst^{+/-}$, $Fstl3^{+/+}$ mice. Although we have not ruled out the possibility that we might see effects of FSTL-3 loss in mice completely lacking follistatin, our data suggest that these two proteins are not functionally redundant in terms of regulating muscle growth. Hence, despite all of the evidence implicating FSTL-3 as a key regulator of myostatin activity *in vivo*, we were unable to uncover any effects of genetic loss of *Fstl3* on muscle mass in these studies.

We also took advantage of the muscle phenotype in $Fst^{+/-}$ mice to investigate genetic interactions between *Fst* and *Mstn*. Our rationale for these studies was that two lines of investigation had demonstrated that other members of the TGF-β family, in addition to myostatin, seem to play important roles in limiting muscle growth. In particular, both overexpression of follistatin as a muscle-specific transgene and systemic administration of a soluble form of one of the known myostatin receptors

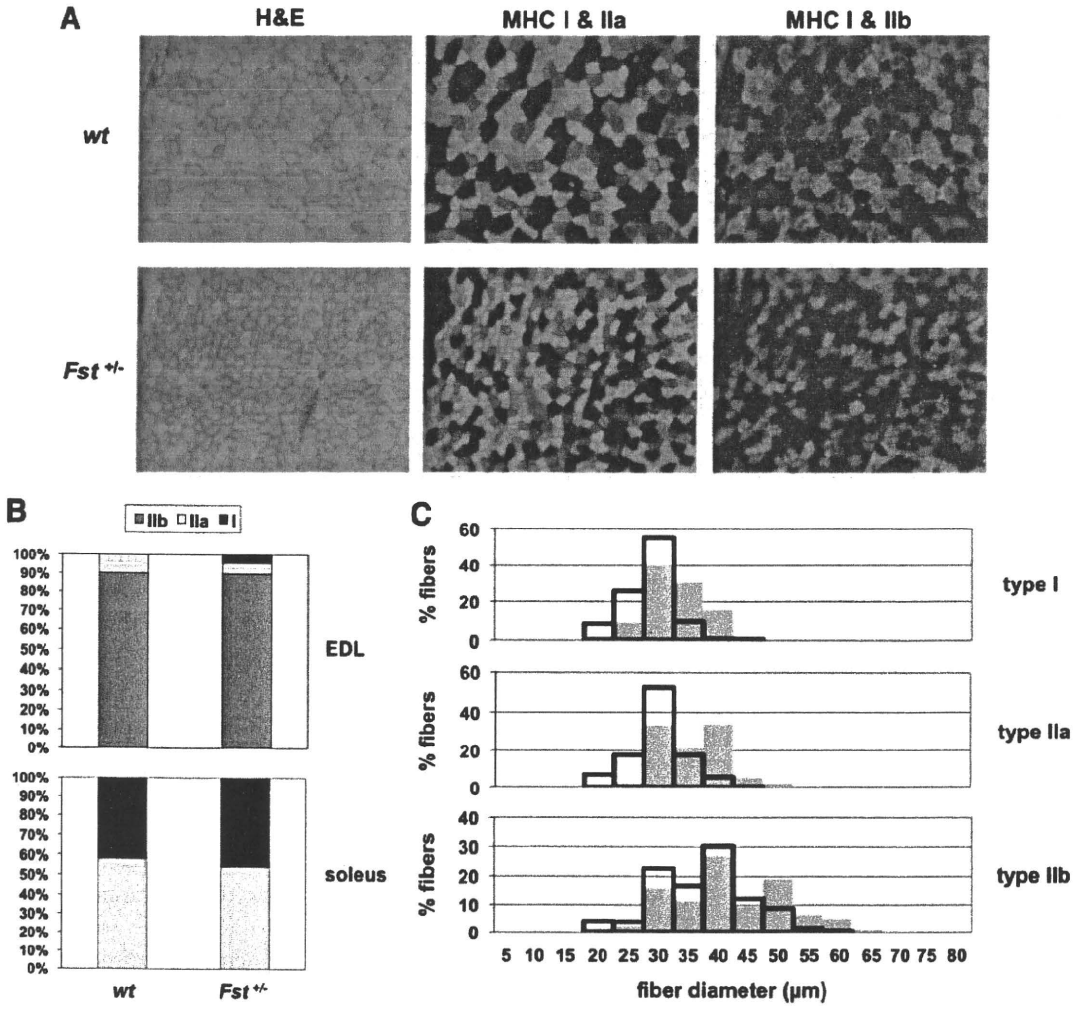

FIG. 2. Fiber type analysis. A, Sections of gastrocnemius muscles either stained with hematoxylin and eosin or incubated with antibodies against type I (*red*), type IIa (*green*), or type IIb (*green*) MHC isoforms. Note that muscles of $Fst^{+/-}$ mice had increased numbers of small, darkly stained fibers, which corresponded to type IIa fibers, as well as increased numbers of type I fibers. B, Fiber type distributions in the EDL and soleus muscles. Note the appearance of type I fibers and the decrease in proportion of type IIa fibers in $Fst^{+/-}$ EDL muscle. C, Distribution of type I, IIa, and IIb fiber diameters in the gastrocnemius muscle. *Solid gray bars* represent muscle fibers from *wild-type* mice, and *open black bars* represent muscle fibers from $Fst^{+/-}$ mice. Note the shift in the distributions toward fibers with smaller diameters in muscles of $Fst^{+/-}$ mice. H&E, hematoxylin and eosin; wt, wild type.

(ACVR2B) had been shown to cause increases in muscle mass not only in *wild-type* mice but also in $Mstn^{-/-}$ mice, implying that these inhibitors were exerting their effects by targeting other TGF-β family members in addition to myostatin (7, 18, 21). Hence, we sought to determine whether the reductions in muscle weights seen in $Fst^{+/-}$ mice result entirely from increased levels of myostatin signaling.

Our approach was to look for genetic interactions between *Fst* and *Mstn* by examining the effect of introducing the *Fst* mutation onto a *Mstn* mutant background. If the sole role for follistatin in regulating muscle mass *in vivo* is to block myostatin signaling, then the *Fst* mutation would be predicted to have no effect in the complete absence of myostatin. If, on the other hand, follistatin normally acts to block multiple ligands to regulate muscle mass, then the *Fst* mutation might be expected to have at least some effect on muscle mass even in a *Mstn* mutant background. As shown in Table 1 and Fig. 1, we found the latter to be the case. Specifically, heterozygous loss of *Fst* caused reductions in muscle mass in both $Mstn^{+/-}$ and $Mstn^{-/-}$ mutant backgrounds in both male and female mice. The effects of the *Fst* mutation were somewhat attenuated in the complete *Mstn*-null background, implying that part of the effect of follistatin loss in $Mstn^{+/+}$ mice likely results from loss of inhibition of myostatin signaling. Nevertheless, the fact that the *Fst* mutation had at least some effect on muscle weights even in the *Mstn*-null background implies that this residual effect resulted from loss of inhibition of other TGF-β family members in these mutant mice. Hence, these studies suggest that follistatin normally acts *in vivo* to inhibit multiple TGF-β family

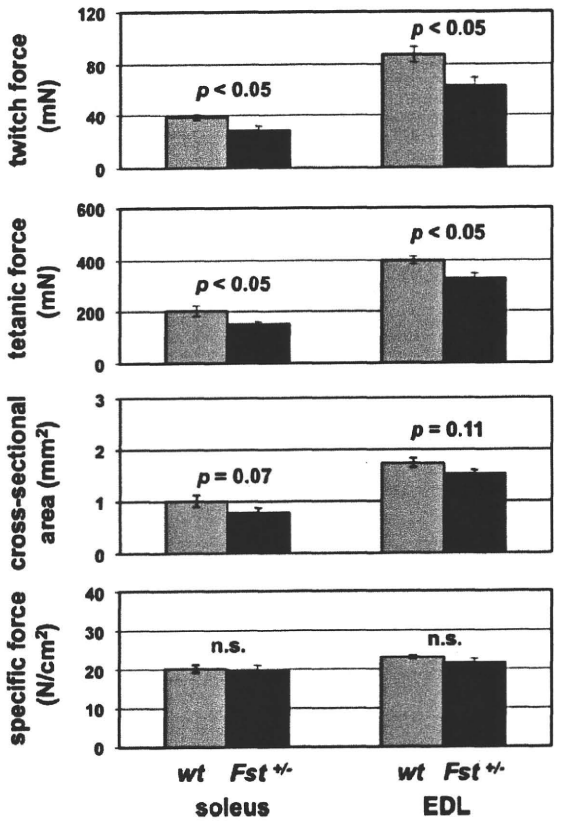

FIG. 3. Force measurements in the soleus and EDL muscles of *wild-type* and $Fst^{+/-}$ mice. Note the decreased twitch and tetanic force with no change in specific force in muscles of $Fst^{+/-}$ mice. n.s., Nonsignificant; $P > 0.20$ wt, wild type.

members, including myostatin, that function to limit muscle mass.

In the final set of experiments, we used genetic approaches to attempt to determine the identity of the ligand (or ligands) that cooperates with myostatin to suppress muscle growth. The TGF-β superfamily consists of almost 40 proteins (for reviews, see Refs 34 and 35), and many could be eliminated as possible candidates based on their known binding properties, because the key ligand can be blocked both by follistatin and by the soluble ACVR2B receptor. The most obvious candidate was growth/differentiation factor (GDF)-11, which is highly related to myostatin and is also expressed in skeletal muscle; genetic studies to date, however, have not revealed any role for GDF-11 in regulating muscle (26). As a result, we decided to extend our genetic analysis to other candidate ligands. The activins, which are dimers of inhibin-β subunits, were attractive as candidates because they had been shown to have *in vitro* activities on muscle cells (36–39). Moreover, a recent study showed that activin A is capable of inducing atrophy when overexpressed in muscle (40).

We decided to focus our initial analysis on mice carrying mutations in genes encoding the inhibin-β subunits. In mice, four genes encoding inhibin-β subunits have been identified, *InhβA*, *InhβB*, *InhβC*, and *InhβE* (for review, see Ref. 34). Mice carrying targeted mutations in each of these genes have been generated and characterized previously (41–44), and for *InhβA* and *InhβB*, we analyzed the existing mutant mouse lines. For *InhβC* and *InhβE*, however, we analyzed a double-mutant mouse line that we generated independently in which the exon encoding the C-terminal domain of *InhβC* and the entire coding sequence of *InhβE* were deleted in the same mutant allele (Fig. 5C). All of these *Inhβ* mutant alleles were backcrossed at least six times onto a C57BL/6 genetic background before analysis.

For the *InhβB* and *InhβC/βE* mutations, we were able to analyze the effect of complete loss of function, as the homozygous mutants are viable as adults. In the case of *InhβA*, however, homozygous loss has been shown to lead to embryonic lethality (43); therefore, we were only able to analyze the effect of heterozygous loss of *InhβA*. As shown in Table 1 and Fig. 5D, the most significant effect that we observed was, in fact, in mice heterozygous for the *InhβA* loss-of-function mutation, which exhibited statistically significant increases in weights of all four muscles that were examined. The effects seen in $InhβA^{+/-}$ mice were most pronounced in males, which had increases ranging from about 8–11%, with P values ranging from 2×10^{-4} to 2×10^{-6} depending on the specific muscle. The effects in females were generally lower, with increases ranging from about 5–8%. These trends were also present after normalizing muscle weights to total body weights (Supplemental Table 1 and Supplemental Fig. 1). Mutations in each of the other genes had little or no effect, except in the case of *InhβB* homozygous mutants, in which two muscles (pectoralis and triceps) also showed statistically significant increases, although the magnitude of the effects was lower than that seen in $InhβA^{+/-}$ mice. These data provide the first loss-of-function genetic evidence that activin A may be one of the key ligands that functions with myostatin to limit muscle mass.

Discussion

Follistatin is a potent myostatin inhibitor that can cause dramatic increases in muscle mass when overexpressed as a transgene in mice (18, 21, 22). Follistatin is known to play an important role in regulating muscle development, because newborn *Fst* mutant mice have a reduced amount of muscle tissue, which is readily discernible by histological analysis (23). Because homozygous *Fst* mutants die immediately after birth, however, little is known about the role that follistatin normally plays in regulating mus-

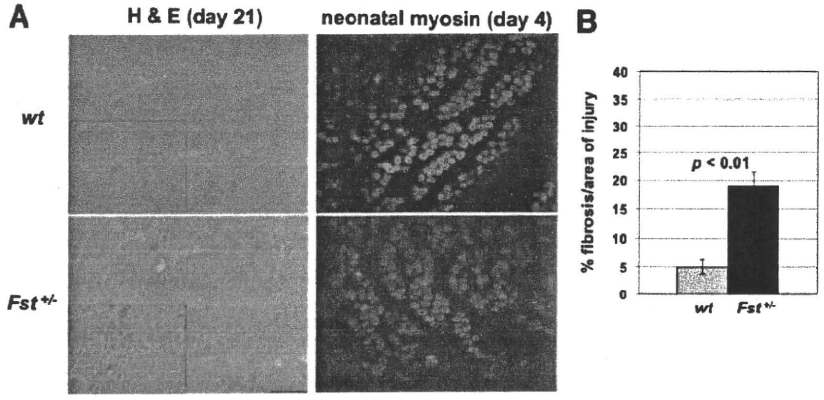

FIG. 4. Impaired muscle regeneration in $Fst^{+/-}$ mice. A, Sections of gastrocnemius muscles of *wild-type* and $Fst^{+/-}$ mice after cardiotoxin-induced injury. At 21 d after injury, note the centrally located nuclei characteristic of regenerating fibers in the *wild-type* injured muscle (see *inset*) and the significantly increased extent of fibrosis in the $Fst^{+/-}$ muscle. At 4 d after injury, note the presence of neonatal myosin in both *wild type* and $Fst^{+/-}$ muscle. B, Quantification of amount of fibrosis at 21 d after cardiotoxin-induced injury as assessed by measurement of percent fibrotic area relative to total injured area. H&E, Hematoxylin and eosin; wt, wild type.

cle homeostasis. Here, we have shown that the *Fst* loss-of-function mutation exhibits haploinsufficiency, with $Fst^{+/-}$ mice having lower overall muscle mass by about 15–20%. These reductions in muscle mass were highly statistically significant and resulted from a shift toward smaller diameter fibers with little or no apparent effect on total fiber number. This shift toward smaller fibers could be attributed to two distinct effects of the *Fst* mutation. First, there was a shift in the distribution of fiber types resulting in an increased proportion of smaller, more oxidative fibers in muscles of $Fst^{+/-}$ mice compared with those of *wild-type* mice. Second, for each fiber type that was examined, there was a shift toward fibers with smaller diameters in muscles of $Fst^{+/-}$ mice compared with those of *wild-type* mice. All of these effects are the opposite of what has been described in mice with absent or reduced myostatin activity, which exhibit increased muscle mass, a shift in fiber types toward more glycolytic fibers, and hypertrophy of both type I and type II fibers (1, 24–27, 45). We also found that $Fst^{+/-}$ mice exhibit an impaired muscle remodeling response to chemical injury, which also contrasts with the enhanced muscle regeneration seen in $Mstn^{-/-}$ mice (for reviews, see Refs. 15–17).

All of these findings demonstrate that follistatin normally functions to suppress activity of this signaling pathway in muscle. In this respect, an important point is that we were able to document significant effects of follistatin loss even though these mice still retained one normal copy of the *Fst* gene. Hence, the effect of follistatin is almost certainly dose dependent, as has been shown for many other components of this regulatory system, and we presume that complete loss of follistatin activity in muscle would lead to much more dramatic effects. We also investigated the possibility that the effects of follistatin loss might have been attenuated by functional compensation by the related protein, FSTL-3. FSTL-3 (also called FLRG) contains two follistatin domains (*vs.* three for follistatin itself), and like follistatin, FSTL-3 is capable of binding and inhibiting both activin and myostatin *in vitro* (31, 46–48) and increasing muscle mass when overexpressed *in vivo* (21, 22). FSTL-3 has been further implicated in the regulation of myostatin based on the fact that FSTL-3 could be detected in a complex with myostatin in both mouse and human blood samples (31). Gene-targeting studies, however, demonstrated that complete loss of FSTL-3 had no effects on muscle mass (32). Using an independently generated *Fstl3*-knockout line, we also observed no effect of homozygous loss of *Fstl3* on muscle mass, and furthermore, we were unable to detect any additive effects of the *Fst* and *Fstl3* loss-of-function mutations. Hence, we were unable to detect any evidence that follistatin and FSTL-3 are functionally redundant with respect to the regulation of muscle mass by myostatin and related proteins.

We also examined genetic interactions between *Fst* and *Mstn*. In particular, we showed that the effects of follistatin loss are seen even in mice null for *Mstn*, implying that myostatin cannot be the sole target for follistatin and that follistatin normally acts to block the activities of multiple TGF-β family members that function to limit muscle mass. These findings are consistent with the results of two prior studies. One set of experiments was the analysis of mice treated with a soluble form of ACVR2B, which has been shown to be one of the activin type II receptors involved in mediating myostatin signaling (7, 18, 49). The soluble form of ACVR2B (ACVR2B/Fc) was shown to be capable of blocking myostatin activity *in vitro*, and administration of ACVR2B/Fc to adult mice was shown to cause dramatic muscle growth (up to 40–60% in 2 wk). Significantly, this effect was attenuated, but not eliminated, in $Mstn^{-/-}$ mice, implying that ACVR2B/Fc was targeting at least one additional ligand that also functions to block muscle growth (7). A second set of experiments was the analysis of transgenic mice overexpressing follistatin in muscle (18). As expected, based on the ability of follistatin to inhibit myostatin, these transgenic mice exhibited significant increases in muscle mass. As in the studies with the soluble ACVR2B receptor, however, the follistatin transgene could also cause increases in muscle

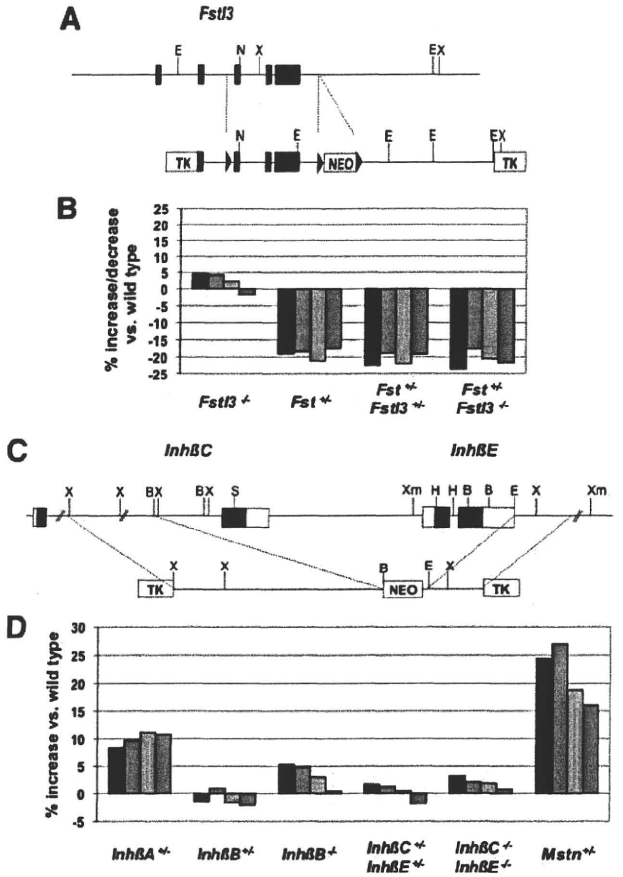

FIG. 5. Effect of a mutation in *Fstl3* and in genes encoding inhibin β-subunits on muscle mass. A, Diagram of *Fstl3*-targeting strategy. Mice carrying the targeted allele were crossed to Ella-cre transgenic mice (33) to generate mice in which recombination had occurred between the outside LoxP sites (denoted by *triangles*), thereby resulting in a mutant allele in which exons 3–5 were completely deleted in the germline. B, Effects of the deletion mutation in *Fstl3* either alone or in combination with heterozygous loss of *Fst*. C, Diagram of *InhβC/InhβE*-targeting strategy. D, Effect of *Inhβ* mutations in male mice. In the *bar graphs* shown in Panels b and d, *numbers* represent percent increase or decrease in muscle mass relative to *wild-type* mice and were calculated from the data shown in Table 1. Data from $Mstn^{+/-}$ mice (21) are shown for comparison. Muscles analyzed were: pectoralis (*red*), triceps (*gray*), quadriceps (*blue*), and gastrocnemius (*green*). TK, Thymidine kinase.

growth even in mice lacking myostatin (21); in fact, the follistatin transgene could cause yet another doubling of muscle mass on top of the doubling seen in the absence of myostatin (*i.e.* an overall quadrupling).

All of these studies demonstrate that at least one other TGF-β family member, in addition to myostatin, also functions to limit muscle mass *in vivo*. Thus, the capacity for increasing muscle growth by targeting this signaling pathway is much more substantial than previously appreciated. We have been using a genetic approach to determining the identity of this other ligand. An obvious candidate was GDF-11, which is highly related to myostatin (1, 50). Initial gene-knockout studies demonstrated that mice completely lacking GDF-11 exhibit multiple developmental defects and die during the perinatal period (51), which precluded a detailed analysis of the role of GDF-11 in muscle. Subsequent studies utilizing a floxed *Gdf11* allele, however, revealed no effect of *Gdf11* deletion specifically in skeletal muscle either alone or in combination with a *Mstn*-knockout mutation (26).

Perhaps the next most likely candidates were the activins, which have been shown to be capable of regulating differentiation of muscle cells in culture (36–39) and share a common receptor with myostatin (for reviews, see Refs. 15 and 34). Moreover, a recent study also suggested the possibility that activins may be involved in regulating muscle mass based on their ability to induce muscle atrophy when overexpressed *in vivo* and based on differential effects seen *in vivo* between follistatin and a follistatin variant with reduced affinity for activin (40). Finally, another recent study implicated activins as well as a number of other ligands, including GDF-11, BMP-9, and BMP-10, as possible candidates based on the fact that these could be affinity purified from serum using the ACVR2B/Fc ligand trap (38). Indeed, by analyzing mouse strains carrying targeted deletions in each of the genes encoding the inhibin β-subunits, we observed increases in muscle mass in mice heterozygous for the *InhβA* mutation, consistent with an important role for activin A in regulating muscle mass. Although further characterization of the muscles of these mice will be required to demonstrate that these effects on muscle mass result from muscle fiber hypertrophy, these data provide the first genetic loss-of-function evidence that activin A may be one of the key ligands that function with myostatin to limit muscle mass.

Although the increases in muscle mass that we observed in *InhβA* mutants were relatively modest, we believe that the overall role that activin A may play is potentially much more substantial for several reasons. First, this phenotype was observed in mice that still retained one functional copy of the *InhβA* gene. By comparison, male mice heterozygous for a mutation in *Mstn* exhibit increases in muscle weights ranging from 16–27% (21); hence, the magnitude of the effects seen in male $InhβA^{+/-}$ mice was approximately half that seen in $Mstn^{+/-}$ mice. Homozygous loss of *Mstn* results in increases in muscle weights of 100–150%, and we presume that greater loss of activin A signaling would similarly result in a significantly enhanced effect. Second, the existence of multiple *Inhβ* genes raises the possibility of functional redundancy, and in this respect, we did see some effect, albeit quite small, in *InhβB* homozygous mutants. Third, a mutation in the *InhβA* gene affects the production of both activin A (as well as activin AB) and inhibin A, which

share the βA-subunit. Given that activins and inhibins generally have counteracting activities, it is perhaps fortuitous that we were able to see any phenotype at all in $Inh\beta A^{+/-}$ mice, because the mutation would lead to decreases in both activin A and an inhibitor of activin signaling. We believe that the likely explanation is that whereas activins are believed to act mostly via a paracrine mechanism, inhibins appear to be capable of regulating signaling in an endocrine manner (for reviews, see Refs. 52–54), and the predominant circulating form of inhibin is known to be inhibin B (for reviews, see Refs. 55 and 56). Hence, the *Inhβ A* mutation would be predicted to reduce levels of activin A but have only a minimal effect on circulating inhibin levels.

Clearly, additional studies will be required to elucidate the precise roles that all of the activin isoforms may play in regulating muscle growth and function in different physiological states. It is interesting to note, however, that circulating levels of activin A in humans have been shown to increase during aging, and conversely, circulating levels of inhibin B have been shown to decrease during aging (57–61), raising the intriguing possibility that enhanced activin signaling during aging may be a key contributing factor in the etiology of age-related sarcopenia. Understanding how muscle homeostasis is coordinately regulated by myostatin and by activins under both normal and pathological conditions will be essential for developing the most optimal strategies to tap the full potential of targeting this general signaling pathway to preserve muscle mass and prevent muscle atrophy in a variety of clinical settings associated with debilitating loss of muscle function.

Materials and Methods

Targeting constructs were generated from 129 SvJ genomic clones and used to transfect R1 embryonic stem cells (kindly provided by A. Nagy, R. Nagy, and W. Abramow-Newerly). Blastocyst injections of targeted clones were carried out by the Johns Hopkins Transgenic Core Facility. All mice were backcrossed at least six times onto a C57BL/6 background before analysis. All analysis was carried out on 10-wk-old mice, except for the force measurements and cardiotoxin studies, which were carried out on 14-wk-old mice. All animal experiments were carried out in accordance with protocols that were approved by the Institutional Animal Care and Use Committees at the Johns Hopkins University School of Medicine and the University of Pennsylvania School of Dental Medicine.

For measurement of muscle weights, muscles were dissected from both sides of the animal and weighed, and the average weight was used. For morphometric analysis, the gastrocnemius muscle was sectioned to its widest point using a cryostat, and fiber diameters were measured as the shortest width passing through the center of the fiber. Measurements were carried out on 84 type I fibers, 150 type IIa fibers, and 150 type IIb fibers per muscle, and mean fiber diameters for each type were calculated for each animal. For plotting the distribution of fiber sizes, data from all three mice in each group were pooled. Measurements were also carried out on 250 fibers of mixed types randomly selected from five representative areas of each section (every attempt was made to analyze the same five regions from muscle to muscle) to estimate overall mean fiber diameters.

For isolated muscle mechanics, mice were anesthetized with ketamine/xylazine. Muscles were removed and placed in a bath of Ringers solution gas equilibrated with 95% O_2/5% CO_2. Sutures were attached to the distal and proximal tendons of the EDL and soleus muscles. Muscles were subjected to isolated mechanical measurements using a previously described apparatus (Aurora Scientific, Ontario, Canada) (62). After optimal length (Lo) was determined by supramaximal twitch stimulation, maximal isometric tetanus was measured in the muscles during a 500-msec stimulation. For histological analysis, samples were rinsed in PBS, blotted, weighed, covered in mounting medium before freezing in melting isopentane, and then stored at −80 C. Muscle cross-sectional areas were determined using the following formula: cross-sectional area = m/(Lo × L/Lo × 1.06 g/cm^3), where m is muscle mass, Lo is muscle length, L/Lo is the ratio of fiber length to muscle length, and 1.06 is the density of muscle (63). L/Lo was 0.45 for EDL and 0.69 for soleus.

For muscle fiber typing, 10-μm frozen cross-sections taken from the midbelly of each muscle were subjected to immunohistochemistry for laminin (rabbit antilaminin Ab-1; Neomarkers, Fremont, CA) to outline the muscle fibers. Fiber typing was performed with antibodies recognizing myosin heavy chain (MHC)2a (SC-71), MHC 2b (BF-F3), and MHC 1 (BAF-8) as previously described (64). Nuclei were counterstained with 4′,6-diamidino-2-phenylindole. Images were acquired on an epifluorescence microscope (Leica, Deerfield, IL) and analyzed for the proportion of myosin-positive fibers using image analysis software (OpenLab, Improvision; Coventry, UK).

For skeletal muscle injury studies, 250 μl of cardiotoxin (10 μM *Naja nigricollis*; Calbiochem, La Jolla, CA) were injected into the gastrocnemius, and muscles were harvested 4 d or 21 d after induction of injury. Quantification of areas of fibrosis per area of muscle injury was performed using Nikon's NIS elements BR3.0 software (Laboratory Imaging; Nikon, Melville, NY).

Acknowledgments

We thank Charles Hawkins and Ann Lawler (Johns Hopkins University School of Medicine) for carrying out the blastocyst injections and embryo transfers and Zuozhen Tian and Magdalena Sikora (University of Pennsylvania School of Dental Medicine) for performing the isolated muscle functional tests.

Address all correspondence and requests for reprints to: Se-Jin Lee, Department of Molecular Biology and Genetics, Johns Hopkins University School of Medicine, 725 North Wolfe Street, Preclinical Teaching Building 803, Baltimore, Maryland 21205. E-mail: sjlee@jhmi.edu.

This work was supported by National Institutes of Health Grants R01AR059685 (to S.-J.L.), R01AR060636 (to S.-J.L.), DP2OD004515 (to R.D.C.), K08NS055879 (to R.D.C.), R01HD32067 (to M.M.M.), and U54AR052646 (to S.-J.L. and

E.R.B.); Muscular Dystrophy Association Grants MDA10065 (to S.-J.L.) and MDA101938 (to R.D.C.), and a gift from Merck Research Laboratories (to S.-J.L.).

Disclosure Summary: Under a licensing agreement between MetaMorphix, Inc. (MMI) and the Johns Hopkins University, S.-J.L. is entitled to a share of royalty received by the University on sales of the factors described in this paper. S.J.L. and the University own MMI stock, which is subject to certain restrictions under University policy. S-J.L., who is the scientific founder of MMI, is a consultant to MMI on research areas related to the study described in this paper. The terms of these arrangements are being managed by the University in accordance with its conflict of interest policies. Y.-.S.L., T.Z., A.S., M.M., K.T., R.D., and E.B. have nothing to declare.

References

1. McPherron AC, Lawler AM, Lee SJ 1997 Regulation of skeletal muscle mass in mice by a new TGF-β superfamily member. Nature 387:83–90
2. Grobet L, Pirottin D, Farnir F, Poncelet D, Royo LJ, Brouwers B, Christians D, Desmecht D, Coignoul F, Kahn R, Georges M 2003 Modulating skeletal muscle mass by postnatal, muscle-specific inactivation gene. Genesis 35:227–238
3. Welle S, Bhatt K, Pinkert CA, Tawil R, Thornton CA 2007 Muscle growth after postdevelopmental myostatin gene knockout. Am J Physiol Endocrinol Metab 292:E985–E991
4. Bogdanovich S, Krag TO, Barton ER, Morris LD, Whittemore LA, Ahima RS, Khurana TS 2002 Functional improvement of dystrophic muscle by myostatin blockade. Nature 420:418–421
5. Whittemore LA, Song K, Li X, Aghajanian J, Davies MV, Girgenrath S, Hill JJ, Jalenak M, Kelley P, Knight A, Maylor R, O'Hara D, Pearson A, Quazi A, Ryerson S, Tan XY, Tomkinson KN, Veldman GM, Widom A, Wright JF, Wudyka S, Zhao L, Wolfman NM 2003 Inhibition of myostatin in adult mice increases skeletal muscle mass and strength. Biochem Biophys Res Commun 300:965–971
6. Wolfman NM, McPherron AC, Pappano WN, Davies MV, Song K, Tomkinson KN, Wright JF, Zhao L, Sebald SM, Greenspan DS, Lee SJ 2003 Activation of latent myostatin by the BMP-1/tolloid family of metalloproteinases. Proc Natl Acad Sci USA 100:15842–15846
7. Lee SJ, Reed LA, Davies MV, Girgenrath S, Goad ME, Tomkinson KN, Wright JF, Barker C, Ehrmantraut G, Holmstrom J, Trowell B, Gertz B, Jiang MS, Sebald SM, Matzuk M, Li E, Liang LF, Quattlebaum E, Stotish RL, Wolfman NM 2005 Regulation of muscle growth by multiple ligands signaling through activin type II receptors. Proc Natl Acad Sci USA 102:18117–18122
8. Grobet L, Martin LJ, Poncelet D, Pirottin D, Brouwers B, Riquet J, Schoeberlein A, Dunner S, Ménissier F, Massabanda J, Fries R, Hanset R, Georges M 1997 A deletion in the bovine myostatin gene causes the double-muscled phenotype in cattle. Nat Genet 17:71–74
9. Kambadur R, Sharma M, Smith TP, Bass JJ 1997 Mutations in myostatin (GDF8) in double-muscled Belgian Blue and Piedmontese cattle. Genome Res 7:910–916
10. McPherron AC, Lee SJ 1997 Double muscling in cattle due to mutations in the myostatin gene. Proc Natl Acad Sci USA 94:12457–12461
11. Grobet L, Poncelet D, Royo LJ, Brouwers B, Pirottin D, Michaux C, Ménissier F, Zanotti M, Dunner S, Georges M 1998 Molecular definition of an allelic series of mutations disrupting the myostatin function and causing double-muscling in cattle. Mamm Genome 9:210–213
12. Clop A, Marcq F, Takeda H, Pirottin D, Tordoir X, Bibé B, Bouix J, Caiment F, Elsen JM, Eychenne F, Larzul C, Laville E, Meish F, Milenkovic D, Tobin J, Charlier C, Georges M 2006 A mutation creating a potential illegitimate microRNA target site in the myostatin gene affects muscularity in sheep. Nat Genet 38:813–818
13. Mosher DS, Quignon P, Bustamante CD, Sutter NB, Mellersh CS, Parker HG, Ostrander EA 2007 A mutation in the myostatin gene increases muscle mass and enhances racing performance in heterozygote dogs. PLoS Genet 3:779–786
14. Schuelke M, Wagner KR, Stolz LE, Hübner C, Riebel T, Kömen W, Braun T, Tobin JF, Lee SJ 2004 Myostatin mutation associated with gross muscle hypertrophy in a child. N Engl J Med 350:2682–2688
15. Lee SJ 2004 Regulation of muscle mass by myostatin. Annu Rev Cell Dev Biol 20:61–86
16. Tsuchida K 2008 Targeting myostatin for therapies against muscle-wasting disorders. Curr Opin Drug Discov Dev 11:487–494
17. Rodino-Klapac LR, Haidet AM, Kota J, Handy C, Kaspar BK, Mendell JR 2009 Inhibition of myostatin with emphasis on follistatin as a therapy for muscle disease. Muscle Nerve 39:283–296
18. Lee SJ, McPherron AC 2001 Regulation of myostatin activity and muscle growth. Proc Natl Acad Sci USA 98:9306–9311
19. Zimmers TA, Davies MV, Koniaris LG, Haynes P, Esquela AF, Tomkinson KN, McPherron AC, Wolfman NM, Lee SJ 2002 Induction of cachexia in mice by systemically administered myostatin. Science 296:1486–1488
20. Amthor H, Nicholas G, McKinnell I, Kemp CF, Sharma M, Kambadur R, Patel K 2004 Follistatin complexes myostatin and antagonises myostatin-mediated inhibition of myogenesis. Dev Biol 270:19–30
21. Lee SJ 2007 Quadrupling muscle mass in mice by targeting TGF-β signaling pathways. PLoS One 2:e789
22. Haidet AM, Rizo L, Handy C, Umapathi P, Eagle A, Shilling C, Boue D, Martin PT, Sahenk Z, Mendell JR, Kaspar BK 2008 Long-term enhancement of skeletal muscle mass and strength by single gene administration of myostatin inhibitors. Proc Natl Acad Sci USA 105:4318–4322
23. Matzuk MM, Lu N, Vogel H, Sellheyer K, Roop DR, Bradley A 1995 Multiple defects and perinatal death in mice deficient in follistatin. Nature 374:360–363
24. Girgenrath S, Song K, Whittemore LA 2005 Loss of myostatin expression alters fiber-type distribution and expression of myosin heavy chain isoforms in slow- and fast-type skeletal muscle. Muscle Nerve 31:34–40
25. Amthor H, Macharia R, Navarrete R, Schuelke M, Brown SC, Otto A, Voit T, Muntoni F, Vrbóva G, Partridge T, Zammit P, Bunger L, Patel K 2007 Lack of myostatin results in excessive muscle growth but impaired force generation. Proc Natl Acad Sci USA 104:1835–1840
26. McPherron AC, Huynh TV, Lee SJ 2009 Redundancy of myostatin and growth/differentiation factor 11. BMC Dev Biol 9:24–32
27. Morine KJ, Bish LT, Pendrak K, Sleeper MM, Barton ER, Sweeney HL 2010 Systemic myostatin inhibition via liver-targeted gene transfer in normal and dystrophic mice. PLoS One 5:e9176
28. McCroskery S, Thomas M, Platt L, Hennebry A, Nishimura T, McLeay L, Sharma M, Kambadur R 2005 Improved muscle healing through enhanced regeneration and reduce fibrosis in myostatin-null mice. J Cell Sci 118:3531–3541
29. Wagner KR, Liu X, Chang X, Allen RE 2005 Muscle regeneration in the prolonged absence of myostatin. Proc Natl Acad Sci USA 102:2519–2524
30. Zhu J, Li Y, Shen W, Qiao C, Ambrosio F, Lavasani M, Nozaki M, Branca MF, Huard J 2007 Relationships between transforming growth factor-β1, myostatin, and decorin. J Biol Chem 282:25852–25863
31. Hill JJ, Davies MV, Pearson AA, Wang JH, Hewick RM, Wolfman NM, Qiu Y 2002 The myostatin propeptide and the follistatin-related gene are inhibitory binding proteins of myostatin in normal serum. J Biol Chem 277:40735–40741
32. Mukherjee A, Sidis Y, Mahan A, Raher MJ, Xia Y, Rosen ED, Bloch KD, Thomas MK, Schneyer AL 2007 FSTL3 deletion reveals

roles for TGF-β family ligands in glucose and fat homeostasis in adults. Proc Natl Acad Sci USA 104:1348–1353
33. **Lakso M, Pichel JG, Gorman JR, Sauer B, Okamoto Y, Lee E, Alt FW, Westphal H** 1996 Efficient *in vivo* manipulation of mouse genomic sequences at the zygote stage. Proc Natl Acad Sci USA 93:5860–5865
34. **Chang H, Brown CW, Matzuk MM** 2002 Genetic analysis of the mammalian transforming growth factor-β superfamily. Endocr Rev 23:787–823
35. **Moustakas A, Heldin CH** 2009 The regulation of TGFβ signal transduction. Development 136:3699–3714
36. **Link BA, Nishi R** 1997 Opposing effects of activin A and follistatin on developing skeletal muscle cells. Exp Cell Res 233:350–362
37. **He L, Vichev K, Macharia R, Huang R, Christ B, Patel K, Amthor H** 2005 Activin A inhibits formation of skeletal muscle during chick development. Anat Embryol (Berl) 209:401–407
38. **Souza TA, Chen X, Guo Y, Sava P, Zhang J, Hill JJ, Yaworsky PJ, Qiu Y** 2008 Proteomic identification and functional validation of activins and bone morphogenetic 11 as candidate novel muscle mass regulators. Mol Endocrinol 22:2689–2702
39. **Trendelenburg AU, Meyer A, Rohner D, Boyle J, Hatakeyama S, Glass DJ** 2009 Myostatin reduces Akt/TORC1/p70S6K signaling, inhibiting myoblast differentiation and myotube size. Am J Physiol Cell Physiol 296:C1258–C1270
40. **Gilson H, Schakman O, Kalista S, Lause P, Tsuchida K, Thissen JP** 2009 Follistatin induces muscle hypertrophy through satellite cell proliferation and inhibition of both myostatin and activin. Am J Physiol Endocrinol Metab 297:E157–E164
41. **Schrewe H, Gendron-Maguire M, Harbison ML, Gridley T** 1994 Mice homozygous for a null mutation of activin β_B are viable and fertile. Mech Dev 47:43–51
42. **Vassalli A, Matzuk MM, Gardner HA, Lee KF, Jaenisch R** 1994 Activin/inhibin βB subunit gene disruption leads to defects in eyelid development and female reproduction. Genes Dev 8:414–427
43. **Matzuk MM, Kumar TR, Vassalli A, Bickenbach JR, Roop DR, Jaenisch R, Bradley A** 1995 Functional analysis of activins during development. Nature 374:354–356
44. **Lau AL, Kumar TR, Nishimori K, Bonadio J, Matzuk MM** 2000 Activin βC and βE genes are not essential for mouse liver growth, differentiation, and regeneration. Mol Cell Biol 20:6127–6137
45. **Cadena SM, Tomkinson KN, Monnell TE, Spaits MS, Kumar R, Underwood KW, Pearsall RS, and Lachey JL** 13 May 2010 Administration of a soluble activin type IIB receptor promotes skeletal muscle growth independent of fiber type. J Appl Physiol 10.1152/japplphysiol.00866.2009
46. **Tsuchida K, Arai KY, Kuramoto Y, Yamakawa N, Hasegawa Y, Sugino H** 2000 Identification and characterization of a novel follistatin-like protein as a binding protein for the TGF-β family. J Biol Chem 275:40788–40796
47. **Maguer-Satta V, Bartholin L, Jeanpierre S, Gadoux M, Bertrand S, Martel S, Magaud JP, Rimokh R** 2001 Expression of FLRG, a novel activin A ligand, is regulated by TGF-β and during hematopoiesis [corrected]. Exp Hematol 29:301–308
48. **Schneyer A, Schoen A, Quigg A, Sidis Y** 2003 Differential binding and neutralization of activins A and B by follistatin and follistatin like-3 (FSTL-3/FSRP/FLRG). Endocrinology 144:1671–1674
49. **Rebbapragada A, Benchabane H, Wrana JL, Celeste AJ, Attisano L** 2003 Myostatin signals through a transforming growth factor β-like signaling pathway to block adipogenesis. Mol Cell Biol 23:7230–7242
50. **Gamer LW, Wolfman NM, Celeste AJ, Hattersley G, Hewick R, Rosen V** 1999 A novel BMP expressed in developing mouse limb, spinal cord, and tail bud is a potent mesoderm inducer in *Xenopus* embryos. Dev Biol 208:222–232
51. **McPherron AC, Lawler AM, Lee SJ** 1999 Regulation of anterior/posterior patterning of the axial skeleton by growth/differentiation factor 11. Nat Genet 22:260–264
52. **de Kretser DM, Hedger MP, Loveland KL, Phillips DJ** 2002 Inhibins, activins and follistatin in reproduction. Hum Reprod Update 8:529–541
53. **Bilezikjian LM, Blount AL, Donaldson CJ, Vale WW** 2006 Pituitary actions of ligands of the TGF-β family: activins and inhibins. Reproduction 132:207–215
54. **Xia Y, Schneyer AL** 2009 The biology of activin: recent advances in structure, regulation and function. J Endocrinol 202:1–12
55. **Robertson DM, Burger HG** 2002 Reproductive hormones: ageing and the perimenopause. Acta Obstet Gynecol Scand 81:612–616
56. **Hurwitz JM, Santoro N** 2004 Inhibins, activins, and follistatin in the aging female and male. Semin Reprod Med 22:209–217
57. **Tenover JS, McLachlan RI, Dahl KD, Burger HG, de Kretser DM, Bremner WJ** 1988 Decreased serum inhibin levels in normal elderly men: evidence for a decline in Sertoli cell function with aging. J Clin Endocrinol Metab 67:455–459
58. **MacNaughton JA, Bangah ML, McCloud PI, Burger HG** 1991 Inhibin and age in men. Clin Endocrinol (Oxf) 35:341–346
59. **Loria P, Petraglia F, Concari M, Bertolotti M, Martella P, Luisi S, Grisolia C, Foresta C, Volpe A, Genazzani AR, Carulli N** 1998 Influence of age and sex on serum concentrations of total dimeric activin A. Eur J Endocrinol 139:487–492
60. **Baccarelli A, Morpurgo PS, Corsi A, Vaghi I, Fanelli M, Cremonesi G, Vaninetti S, Beck-Peccoz P, Spada A** 2001 Activin A serum levels and aging of the pituitary-gonadal axis: a cross-sectional study in middle-aged and elderly healthy subjects. Exp Gerontol 36:1403–1412
61. **Bohring C, Krause W** 2003 Serum levels of inhibin B in men of different age groups. The Aging Male 6:73–78
62. **Barton ER, Morris L, Kawana M, Bish LT, Toursel T** 2005 Systemic administration of L-arginine benefits mdx skeletal muscle function. Muscle Nerve 32:751–760
63. **Brooks SV, Faulkner JA** 1988 Contractile properties of skeletal muscles from young, adult and aged mice. J Physiol 404:71–82
64. **Schiaffino S, Salviati G** 1997 Molecular diversity of myofibrillar proteins: isoforms analysis at the protein and mRNA level. Methods Cell Biol 52:349–369

基礎老化研究　34(4);5－11,2010

【総　説】

老化や疾患における骨格筋の萎縮と治療への応用

上住　聡芳、中谷　直史、常陸　圭介、土田　邦博
藤田保健衛生大学・総合医科学研究所・難病治療学研究部門

要約

老化や難治性筋疾患等に伴って、骨格筋は形態的変化および機能低下が生じる。老化では特に速筋型のタイプII筋線維の萎縮が顕著に見られ、脂肪沈着や繊維化が見られる。骨格筋の再生を担うのは筋衛星細胞であるが、老化に伴い、筋再生能力の低下を来たす。近年、骨格筋量調節因子であるマイスタチンやアクチビンの機能制御により、筋萎縮が防げる事が明らかとなってきた。マイスタチン阻害によって、筋萎縮の防止、繊維化の抑制、体脂肪量の減少、脂肪肝抑制が期待されており、老化、筋疾患、悪液質への応用も現実味を帯びてきた。更に、脂肪細胞の起源に関する研究に近年大きな進展があり、骨格筋内の異所性脂肪変性を担う細胞群や脂肪組織での脂肪産生細胞の起源が明らかとなってきた。本総説では、老化、筋疾患等に伴って生じる筋萎縮の病態と治療法開発の現状、そして、脂肪細胞の起源と異所性脂肪変性に関する最新の知見を筆者らの研究を中心に紹介する。

キーワード：sarcopenia, muscle atrophy, myostatin, muscular disease, ectopic fat formation

1. はじめに

筋骨格系は、骨格筋、腱、骨、軟骨、脂肪組織、結合組織から構成され、生体の最重量を占める組織である。とりわけ、骨格筋は成人の身体中の重量の約40%を占め、関節運動を協調させた円滑な運きや姿勢の維持に関与している。熱産生による体温の維持やインスリンの標的臓器として血糖調節にも重要な役割を果たしている。骨格筋は、老化や各種病態によって劇的な変化と機能低下を示す。筋骨格系組織の機能低下は、運動能力低下に直結し、日常生活動作（ADL）や生活の質（QOL）を低くするため、その対策は医学的に重要である。

骨格筋は、筋膜に包まれた筋線維と結合組織で構成されている。筋線維は、多くの筋芽細胞が融合した結果、多核を形成する筋細胞で形成されるが、分裂して新たな筋線維を生み出す事は出来ない。その役割を担うのは、筋線維の基底膜直下に存在する単核の筋衛星細胞（サテライト細胞）である。筋衛星細胞は骨格筋の発生に寄与すると共に、筋線維の損傷時には、増殖、分化、融合といった経過をたどり、筋再生に重要な働きをしている。筋線維は、遅筋線維（タイプI）と速筋線維（タイプIIA, IIB, IIX）に分けられ、遅筋線維はミトコンドリアを豊富に含み、酸化系酵素の活性が高く、収縮速度は遅いが疲労しにくい性質を持つ。ミオグロビンを多く含み赤筋線維とも呼ばれる。速筋線維は、解糖系酵素活性が高く収縮速度は早いが、特にIIB, IIX線維は疲労しやすい。無酸素状態での代謝に依存しており、白筋線維とも呼ばれる。

脊髄前角に細胞体を持つα運動ニューロンとそれに支配される筋線維を運動単位と呼ぶ。身体内には400を超える骨格筋が存在し、遅筋線維と速筋線維が混在しているがそれぞれの骨格筋では、その比率は異なっている。トレーニング等で、筋線維を肥大させたり、線維タイプをIIB型からIIA型への変換させることで持久力を改善させる事は可能と考えられている。

骨格筋組織は生体内で隣接する骨格筋内の細胞のみならず、身体内の脂肪組織や内臓臓器、神経組織との間で、サイトカインの産生と受容、神経連絡を介して相互連携しており、生体の恒常性維持に重要な役割を果たしている。

最近の研究で、老化や筋疾患によって生じる筋萎縮を抑制可能であることが示されている。特に、骨格筋から産生されるマイオスタチンと呼ばれる分子を阻害する治療法は、有望視されている。骨格筋は、再生医療の分野からのアプローチも期待されている。骨格筋は再生能力の高い組織であり、筋衛星細胞が筋再生に大きな役割を担っている。筋衛星細胞以外にも独特の分化能や特徴を持った前駆細胞が存在し、骨格筋の恒常性維持に寄与している。本総説では、骨格筋の老化や疾患における変化を述べると共に、筋萎縮の防止法や最近発見された脂肪前駆細胞群について紹介する。

連絡先：〒470-1192
愛知県豊明市沓掛町田楽ヶ窪1-98
Tel: 0562-93-9384
Fax: 0562-93-5791
E-mail: tsuchida@fujita-hu.ac.jp

2. 骨格筋の形成と筋萎縮

1) 骨格筋の形成

横紋筋である骨格筋は、胎児期の体節に由来し、体節中の筋前駆細胞が運命決定され筋分化に寄与している。筋前駆細胞は遊走と増殖を行ない、細胞融合と成熟過程を経て多核の筋線維を形成する。Helix-loop-helix構造を持ったMyoDファミリー転写因子群が骨格筋の分化制御に決定的な役割を果たしており、筋分化決定因子(muscle determining factor, MRF)と呼ばれる。MyoDとMyf5は主として筋芽細胞への分化決定と維持に働き、myogeninとMRF4は主に筋芽細胞から筋管細胞への最終分化に関与する [1]。

Pax7は、胚期や周産期の骨格筋形成に必須の分子であり、生後は筋衛星細胞の生存に必須であると考えられている [2]。筋衛星細胞は、筋細胞の筋形質膜と基底膜の間に存在し、成体の筋再生を担う細胞であり、Pax7は筋衛星細胞のマーカーとして頻用されている。胎生期の皮筋節のPax3/Pax7陽性細胞が筋衛星細胞の起源であることが示されている [2]。長らく、Pax7の筋衛星細胞での発現が筋再生に必須であると考えられていたが、マウスの実験から、生後2-3週以降では、Pax7は筋衛星細胞による筋再生に必須ではない事が示された [3]。なお、試験管内で、筋分化を示す細胞には、筋衛星細胞以外に、骨髄等の間葉系幹細胞、血管由来の前駆細胞、iPS細胞等がある。

2) 骨格筋形成におけるマイオスタチンの役割

生体内の個々の組織の大きさを決定するための抑制因子が存在するという仮説があり、カローン仮説と呼ばれている [4]。骨格筋のカローンの最有力候補が骨格筋から産生され筋量を負に制御しているマイオスタチンである。マイオスタチンは、1997年に機能が明らかになったTGF－βファミリーに属するサイトカインである [5]。マイオスタチンが遺伝子変異等で欠損したり、マイオスタチン阻害分子を投与すると、骨格筋量が増大する。遺伝子破壊マウスやウシ、羊、Whippetと呼ばれる短距離レースの犬などで遺伝子レベルでのマイオスタチン阻害動物の例が報告されている [5-8]。羊の場合は、マイオスタチン遺伝子の3'翻訳領域が変異することで、骨格筋特異的なmiRNAであるmiRNA1やmiRNA 206の標的部位となることで、発現が減少する [8]。ヒトのマイオスタチン変異も報告されており、筋量と筋力が増大し脂肪量が少ない [9]。マイオスタチンが筋量を調節する詳細な分子機構は不明点も多いが、筋線維構成分子のタンパク分解系の亢進が作用機構の一つだと想定されている。マイオスタチン阻害は、筋衛星細胞の分化調節へ影響を及ぼすが、その寄与は当初考えられていたより少ないとする報告もある [10,11]。マイオスタチンとタンパク質の一次構造上類似したアクチビンAも筋量の調節に関与している [12]。マイオスタチンの作用が骨格筋に特異的であるのに比較して、アクチビンの作用は全身におよぶ。アクチビンは下垂体からの卵胞刺激ホルモンの分泌作用を基に精製されたホルモンであるが、生殖系への作用以外にも、神経栄養因子としての作用や記憶への関与など多彩な作用を有している [13]。アクチビンとマイオスタチンの阻害分子としてホリスタチン（FSTN）が知られている [14]。我々は、FSTNに由来しアクチビンへの阻害がないマイオスタチン阻害因子を開発した [15]。開発因子やFSTNには成体の筋量を増加させる効果がある [15,16]。FSTN等のマイオスタチン阻害因子の遺伝子導入や因子の投与で筋量を増大させ、筋ジストロフィーモデル動物の病態を軽減可能である事が確認されている [15,16]。

3) 骨格筋萎縮の分子機構

骨格筋萎縮は、筋肉構成タンパク質の合成と分解の正常なバランスが崩れた状態で引き起こされる。老化に伴う筋萎縮はサルコペニア（sarcopenia）と呼ばれる。加齢の初期の筋萎縮には、筋自体の寄与が大きい。形態学的には、筋線維数は加齢に伴って40%もの減少が見られる。横断面積の縮小もII型筋線維に顕著に見られ、I型とII型筋線維が混在した筋線維が増える。また、同系統の筋線維が束になって存在する筋線維のグループ化が生じる。この原因としては、高齢者ほど運動単位数が減少する事による神経原性変化に起因する事が示唆されている。つまり、老化では、筋原性萎縮と運動単位の減少による神経原性変化の両者が生じる。さらに、細胞死も関与すると考えられている。サルコペニアの特徴は、ゆっくりと筋力や筋持久力が低下していく事である。一方、重症の脊椎損傷による半身麻痺や脳梗塞などで長期の寝たきり（ベッドレスト）やギブス固定で生じる筋萎縮は廃用性筋萎縮と呼ばれるが、遅筋型のタイプI線維が優位に萎縮し、速筋優位となる。

筋萎縮は、加齢に伴って生じる以外にも、筋ジストロフィーを代表とする遺伝性の神経筋疾患で見られる。さらには、癌や感染症、慢性心不全、肝不全の末期に生じる悪液質（カヘキシー、cachexia）では、筋萎縮と共に脂肪細胞の萎縮が生じて体の恒常性が維持出来ない。悪液質では、食思不振、体重減少、栄養障害、疲労が見られる。TNFαやIL-6などのサイトカインの発現の変化が病態に関与するが、現状では治療法は存在しない。

蛋白質分解系には、ライソソーム系、カルパイン系、ユビキチン／プロテアソーム系があるが、骨格筋萎縮では、筋特異的ユビキチンリガーゼの発見がなされ、主にユビキチン／プロテアソーム活性の上昇によるタンパク分解の亢進の解析が大きく進展した [17]。MuRF1(muscle RING finger-1)とMAFbx-1/atrogin-1は、坐骨神経切断等の筋萎縮で発現上昇する骨格筋と心筋特異的なユビキチンリガーゼであり、筋萎縮時に活性化する [17]。これらの遺伝子破壊マウスや阻害で、筋萎縮に抵抗性を示す事から筋萎縮を担う重要分子であると考えられている [17]。IGF-1 (insulin-like growth factor-1)は強力に筋形成を促すが、その下流で、Akt-1がリン酸化により活性化する。Akt-1が活性化すると、S6キナーゼ系によりタンパク質合成が上昇すると共に、転写因子のFOXO (forkhead box O)がリン酸化する。リ